

Ultra-deep Imaging: Structure of Disks and Haloes

Johan H. Knapen and Ignacio Trujillo

Abstract Deep imaging is a fundamental tool in the study of the outermost structures of galaxies. We review recent developments in ultra-deep imaging of galaxy disks and haloes, highlighting the technical advances as well as the challenges, and summarizing observational results in the context of modern theory and simulations. The deepest modern galaxy imaging comes from three main sources: (1) surveys such as the Sloan Digital Sky Survey's Stripe 82 project, (2) very long exposures on small telescopes, including by amateurs, and (3) long exposures on the largest professional telescopes. The technical challenges faced are common in all these approaches, and include the treatment of light scattered by atmosphere and telescope/instrument, correct flat fielding, and the subtraction of non-galaxy light in the images. We review scientific results on galaxy disks and haloes obtained with deep imaging, including the detection and characterization of stellar haloes, tidal features and stellar streams, disk truncations, and thick disks. The area of ultra-deep imaging is still very much unexplored territory, and future work in this area promises significant advances in our understanding of galaxy formation and evolution.

1 Introduction

Our knowledge of the properties of disks of galaxies has been driven by deep imaging for the past decades. Until the mid-1980's, such imaging was done with photographic plates, prepared using specialist chemical techniques and then exposed for long times on large telescopes, often by observers spending long and uncomfortable hours in the prime focus cage of the telescope. The early history of this, and the subsequent physical parameters derived for disk galaxies, have been summarized

Johan H. Knapen and Ignacio Trujillo
Instituto de Astrofísica de Canarias, E-38200 La Laguna, Spain and Departamento de Astrofísica,
Universidad de La Laguna, E-38206 La Laguna, Spain, e-mail: jhk@iac.es and e-mail:
trujillo@iac.es

by, e.g., van der Kruit and Freeman (2011). Main findings relating to the structure of disks include the description of the surface brightness distribution of disks as exponential by Freeman (1970), and the realization that the vertical profiles of disks seen edge-on can be described by an isothermal sheet (van der Kruit and Searle 1981). Although in the early days they were limited by a small field-of-view (FOV) and flat fielding issues, imaging with charge-coupled devices (CCDs) quickly took over from photographic plates. Large imaging surveys now provide most data, as reviewed below.

A powerful alternative to deep imaging of integrated light from galaxies is imaging and characterizing individual stars in the outskirts of a galaxy, either by using a camera with a large FOV to observe Local Group galaxies like M31, or by using the *Hubble Space Telescope* (*HST*) to observe dwarf galaxies in the Local Group or to resolve the stars in galaxies outside the Local Group but at distances smaller than 16 Mpc (Zackrisson et al 2012). Exploration in this sense of M31 started with the Isaac Newton Telescope Wide Field Camera survey (Ibata et al 2001) and has been recently reviewed by Ferguson and Mackey (2016). Key references for other nearby galaxies include Dalcanton et al (2009); Radburn-Smith et al (2011); Gallart et al (2015) and Monachesi et al (2016). In the current Chapter, we will concentrate on imaging of integrated light, and refer the interested reader to the Chapter by Crnojevic (this volume) for a review of results based on imaging individual stars.

Over the past decade, advances in detector technology, observing strategies, and data reduction procedures have led to the emergence of new lines of research based on what we call here ultra-deep imaging. This can be obtained in large imaging surveys, or obtained for small samples of galaxies, or for individual ones, using very long exposure times on small telescopes, or with large professional telescopes. In this Chapter, we will give examples of the first and third category, whereas impressive examples of results from the second category can be found in the Chapter by Abraham et al (this volume).

In this Chapter, we will first discuss the various challenges that need to be overcome before ultra-deep imaging can be used to distill scientific advances, in particular those due to light scattered in the atmosphere and telescope, flat fielding, and sky subtraction. We will then briefly review the main approaches to obtain deep imaging, namely from imaging surveys, using small telescopes, and using large professional telescopes. In Sect. 4, which forms the heart of this review, we consider the progress in our understanding of the outskirts of galaxies that has been achieved thanks to ultra-deep imaging, paying particular attention to the properties of galaxy disks (including thick disks and disk truncations) and stellar haloes, but also touching on properties of tidal streams and satellites. When concluding, we will describe future developments, challenges and expected advances.

2 The Challenges of Ultra-deep Imaging

Obtaining ultra-deep imaging of the sky is plagued with difficulties. For this reason going beyond the $30 \text{ mag arcsec}^{-2}$ frontier (approximately 1500 times fainter than the darkest sky on Earth) has remained rather elusive. In this Section, we review the most important challenges that need to be addressed carefully if one desires to obtain ultra-deep imaging.

2.1 Sky Brightness

Professional astronomical observatories are located on the darkest spots on Earth. Even at these locations (where light pollution caused by human activity is minimal) the night sky brightness is substantial: $\mu_V \sim 22 \text{ mag arcsec}^{-2}$. This brightness is mainly due to various processes in the upper atmosphere, such as the recombination of atoms which were photoionized by the Sun during the day, a phenomenon known as airglow. With long enough integrations we are able to reduce the noise in this brightness which results from the intrinsic variability of the night sky, and easily obtain images in which we can measure features which are much fainter than the intrinsic sky brightness. However, the sky brightness also contains other components. Beyond our atmosphere, a diffuse light component is caused by the reflection of sunlight on the dust plane of our Solar system. This is the zodiacal light, with a brightness of around $\mu_V \sim 23.5 \text{ mag arcsec}^{-2}$. This brightness affects particularly those regions of the sky around the ecliptic plane and it contaminates all observations, including those obtained with space telescopes. The intensity of the zodiacal light is variable and depends on the Solar activity.

2.2 Internal Reflections

Internal reflections are due to the structure of the telescope and the dome. These reflections can appear at different surface brightness levels but are quite common when one reaches levels of $\mu_V \gtrsim 26 \text{ mag arcsec}^{-2}$. There are two approaches to minimize these reflections. One way is to use telescopes with simple optics (Abraham and van Dokkum 2014; see also Abraham et al, this volume), another is to implement clever observing strategies which avoid repetition of similar orientation of the camera on the sky (e.g., Trujillo and Fliri 2016).

2.3 *Flat Fielding*

To obtain reliable ultra-deep imaging, an exquisite flat field correction of the images needs to be performed. This correction is needed to ensure that a uniform illumination of the CCD leads to a uniform output, or uniform counts in the image. In a CCD camera, this is not the case by default as the gain and dark current change across the face of the detector, and distortions due to optics can cause non-uniformities. The process of flat fielding removes all these pixel-to-pixel variations in sensitivity and the effects of distortions in the optical path. Flat field images are often obtained by exposing on uniformly illuminated surfaces.

Any artefact (gradient, pattern, etc.) left behind during the process of creating the flat field image used to correct the raw science images will introduce a systematic error in the final image, which in turn will prevent reaching the expected surface brightness limit of the observation. The key to creating a good flat field image is to have a uniform illumination of the CCD of the camera. For most observing cases, a twilight (or even a dome) flat is good enough for this purpose. However, when the goal is to reach very faint details of the image a different approach is needed, consisting in creating a flat field using the night sky imaging itself. Such a flat field, using a set of science images, is sometimes referred to as a master flat.

To create a good master flat, the set of science images must be taken at different locations on the sky. In fact, depending on the apparent size of the galaxy, the displacement between one science image and the next should be at least as large as the size of the object. Ideally, not all the science images of a specific galaxy should be located at the same position on the CCD (and, ideally, should also not have the same position angle on the sky). That means preparing an observing scheme that includes both a dithering and a rotation pattern (see the example of this procedure in Trujillo and Fliri 2016). In addition, if the observations are taken over different nights (or observing blocks), the best approach is to create a master flat for each night (or observing block). The use of all the science images in a run rather than those of a single night or observing block is not generally a good idea as slight differences from night to night in the focus and the vignetting correction hinder such an approach.

Once all the science images have been acquired, the process of building a master flat is as follows. First, all the objects in each individual science image are generously masked (for instance using SExtractor; Bertin and Arnouts 1996). Only the pixels outside the masked areas are used to create the final master flat. Second, to guarantee that all the science images are appropriately weighted during their combination to create the master flat, every individual science image of a given night is normalized. Finally, the normalized and masked individual science images are median-combined into a single master flat.

2.3.1 Drift Scanning

An alternative approach which has been used to achieve high-quality flat-fielding is referred to as drift scanning, or a variant on this called time delay and integration (TDI; McGraw et al 1980; Wright and Mackay 1981). In drift scanning, the reading of the CCD is done at the same slow rate as the CCD is moved across the sky. In TDI, the CCD does not move, but the readout is timed to coincide with the sidereal rate at which the sky passes by. In both cases, an object is sampled by every pixel in a column, thus averaging out all defects and achieving an extremely efficient flat fielding. As in the case of the masterflat described above, the background itself is used for flat fielding, assuring a perfect colour match. Further details, as well as a more complete historical overview, are given by Howell (2006).

In practice, in spite of these significant advantages, drift scanning or TDI have not been used much in the literature. The reasons for this vary, but include the difficulty of adjusting the relative movement of sky and CCD with the readout, the loss of efficient observing during the ramp-up and ramp-down phases at the start and end of an exposure, image elongation effects, and the fact that the exposure time is fixed by the telescope+CCD setup, and often rather short.

In the field of imaging nearby galaxies, the most notable exception to this general dearth of TDI results is the Sloan Digital Sky Survey (SDSS, York et al 2000). As described by Gunn et al (1998)¹, the SDSS large-format mosaic CCD camera has been designed to image strips of the sky simultaneously in five colour bands using the TDI technique. The approach chosen by the SDSS team has proven to be very successful in terms of imaging to low surface brightness levels. Even though the exposure time of SDSS images is less than one minute (53.9 s) and the telescope of modest size (2.5 m), the exquisite flat fielding and sky background allow one to reach very low surface brightness levels indeed, down to $26.5 \text{ mag arcsec}^{-2}$ (3σ in an area of $10 \times 10 \text{ arcsec}$; Trujillo and Fliri 2016) or down to $27.5 \text{ mag arcsec}^{-2}$ when analyzing elliptically averaged surface brightness profiles (see, e.g., Pohlen and Trujillo 2006). As illustrated in Sect. 3, co-adding series of SDSS images, as is possible in the Stripe 82 survey area, brings that level down by another $2 \text{ mag arcsec}^{-2}$, allowing ground-breaking science to be performed.

2.4 Masking and Background Subtraction

Deep images often reveal coherent structure at low levels, which can be due to, e.g., imperfect flat fielding, spatial variations in the background sky, or residual point spread function (PSF) effects. Deep images of galaxies also show foreground stars, as well as background galaxies. All these components must be identified, taken into account, and/or subtracted before a deep galaxy image can be analysed. As an example of the procedures followed, we show in Fig. 1 a SDSS Stripe 82 image of

¹ For a more detailed description of the flat field procedures used by the SDSS, see <http://classic.sdss.org/dr5/algorithms/flatfield.html>.

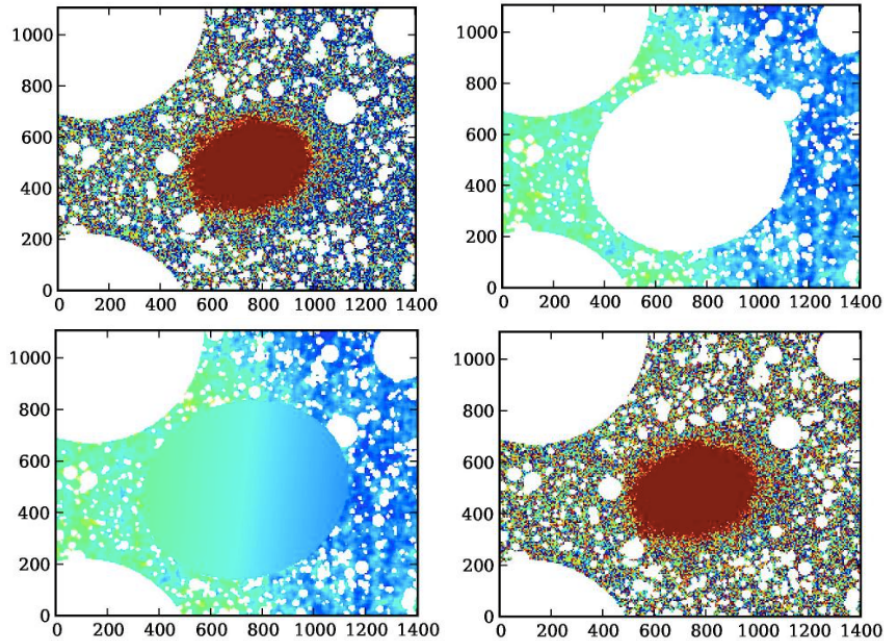


Fig. 1 Example of residual background modelling and subtraction, for a Stripe 82 image of the galaxy NGC 941. *Top left* panel: original image, showing a gradient in the background level. White areas are masked-out images of foreground stars and background galaxies. Image labels are in pixels, with size 0.396 arcsec. North is right, East to the bottom. *Top right*: model for the background, excluding the area of the galaxy. *Lower left*: background model, extrapolated over the area of the galaxy. *Lower right*: final image, with the background model subtracted from the original. Reproduced with permission from Peters et al (2017)

NGC 941 as analysed by Peters et al (2017). Stars and background galaxies are generously masked, after which a polynomial two-dimensional fit is made to the remaining background pixels. In our example, this is dominated by a left-right gradient in the background level, but the fit also shows smaller-scale structure. The latter could, in principle, be real structure, either related to the galaxy (e.g., tidal streams) or not (e.g., Galactic cirrus, see Sect. 2.6). If one looks for structure like tidal streams a different background modelling technique must be used, for instance only modelling large-scale fluctuations or gradients. This neatly highlights the difficult nature of this kind of analysis.

In our example, the gradient in the background in all probability is also present at the location of the galaxy, which is why we extrapolate the background model into the galaxy region (lower left panel of Fig. 1). This model is then subtracted from the original image, and the result can be used for scientific analysis, in this case studying the shape of the outer regions through analysis of azimuthally averaged radial profiles (see Sect. 4.2; this is why the small-scale background structure described in the previous paragraph could safely be subtracted off in this case). The

uncertainty limit, down to which these radial profiles can be trusted, is just below $30 \text{ mag arcsec}^{-2}$ for the image shown in Fig. 1 (data taken from the IAC Stripe82 Legacy Project; Fliri and Trujillo 2016).

2.5 Scattered Light

A further and important source of background contamination is produced by all the emitting sources in the image (or even just outside the imaged area). The light of these sources is scattered by the PSF of the instrument across the entire image. Slater et al (2009) have shown that at $\mu_V \sim 29.5 \text{ mag arcsec}^{-2}$, an image taken from the ground has all its pixels affected by scattered light from nearby bright sources. Properly removing this contamination is quite challenging, and requires an extremely accurate characterization ($<1\%$ at large distances) of the PSF of the camera.

The excess light redistributed by the PSF from both the object of interest and the nearby surrounding sources creates a two-dimensional and highly structured surface that is the main contributor to the background of the image at the faintest surface brightness levels ($\mu_V \gtrsim 29 \text{ mag arcsec}^{-2}$, Slater et al 2009). All astronomical images are affected by this scattered light background which is the result of the convolution of the PSF with the light of the sources. The scattered light background of an astronomical image will be more intense if the number of bright sources in the image is large and also if the PSF has significant wings. In this sense, the best option (if feasible) is to select a target within a field devoid of nearby bright surrounding objects. A typical scattered light background is illustrated in Fig. 2.

Figure 2 illustrates how to deal with the background of scattered light. First, the PSF must be characterized as perfectly as possible by using a reliable extended PSF. An extended PSF with high a signal-to-noise ratio in its outer wings will allow the exploration of the distribution of the light of the nearby brightest sources up to the position of the galaxy under exploration. Second, using the extended PSF a background scattered light map is created. If the main contributor to the scattered light background is the presence of bright stars then the scattered light map is created by simply locating the model PSF at the position of the bright stars and scaling the flux of the PSF to these bright sources. Finally, the scattered light map is subtracted from the observed image.

Above, we have discussed the effect of the scattered light created by the surrounding sources around the galaxy of interest. Naturally, the light distribution of the object itself is also convolved with the PSF. In this sense, the scattered light of the targeted galaxy is also creating an artificial excess of light in the outermost region of the galaxy that needs to be addressed in order to explore the properties of the object in its outer regions. We illustrate how to deal with this in Sect. 4.4.1 of this Chapter.

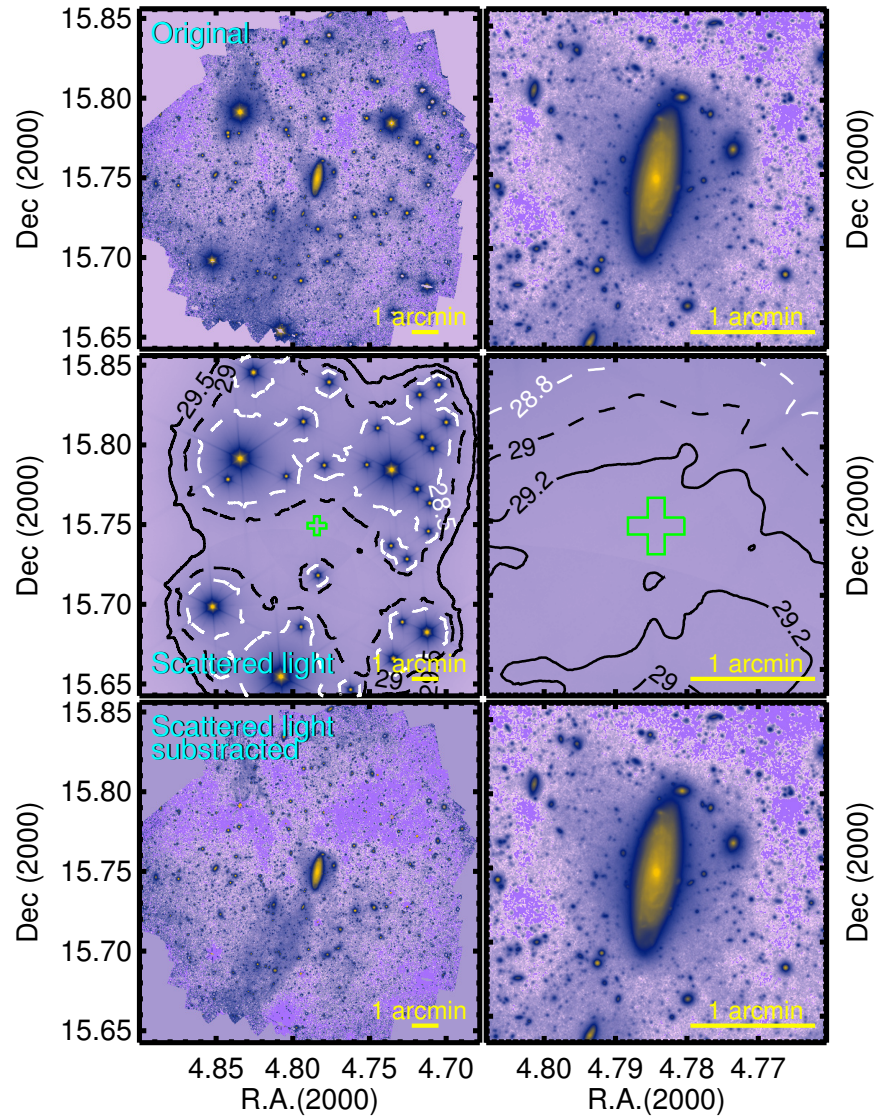


Fig. 2 The scattered light around the galaxy UGC 00180 produced by all the stars brighter than $R = 17$ mag in its vicinity. *Top row*: original field (left) and a zoom-in of the galaxy. *Middle row*: scattered light. The position of the galaxy is illustrated with a green cross. Contours of surface brightness are 28.5, 29, and 29.5 mag arcsec⁻² (left) and 28.8, 29, and 29.2 mag arcsec⁻² (right). *Lower row*: original field after subtraction of the scattered light produced by the brightest sources. Figure taken from Trujillo and Fliri (2016), reproduced with permission of the AAS

2.6 Galactic Cirrus

Finally, if one is interested in exploring the fainter structures of galaxies, the presence of Galactic cirrus in the images needs to be considered. These filamentary structures are located everywhere on the sky, even at higher Galactic latitudes. For this reason, a careful preselection of the fields to be observed is necessary to minimize the contamination by cirrus. A good illustration of the perils of Galactic cirrus is presented by Davies et al (2010) for the case of the M81 group. They found that far-infrared emission measured by the *Herschel* satellite correlates very well spatially with narrow-velocity Galactic HI, without any evidence that this far-infrared emission originates in the M81 group. They thus inferred that the optical streams and structures seen in the M81 group are not in fact part of the group, but are rather due to light from our own Galaxy which is back-scattered off Galactic dust.

3 Approaches in Ultra-deep Imaging

The last few years have seen an explosion in the number of works exploring the outermost regions of nearby galaxies using very deep imaging. These works can be grouped into three different flavours: deep (~ 1 h) multipurpose surveys with medium sized (2 – 4 m) telescopes, extremely long integrations ($\gtrsim 20$ h) of particular galaxies with small ($\lesssim 1$ m) telescopes or long integrations ($\gtrsim 5$ h) with large ($\gtrsim 8$ m) telescopes. In what follows we will summarize some of these efforts.

3.1 Survey Data

The 3.6 m Canada-France-Hawaii Telescope (CFHT), with its MegaCam wide-field camera comprising 36 CCDs and covering a 1 square degree FOV, has played a significant role in the new generation of deep imaging surveys. This telescope has been used for general purpose surveys like the Wide Synoptic CFHT Legacy Survey (155 square degrees; Cuillandre et al 2012), or more specific projects like the Next Generation Virgo Cluster Survey (NGVCS; Ferrarese et al 2012) or the deep imaging follow-up (Duc et al 2015) of the ATLAS^{3D} project (Cappellari et al 2011). These surveys are characterized by having similar depths ($r \sim 25 - 25.5$ mag; $S/N = 10$ for point sources) using integration times of 40 – 60 min, reaching a limiting surface brightness of $28.5 - 29$ mag arcsec⁻² (3σ in 10×10 arcsec²).

Among the most important results of the NGVCS is the connection between the distribution of the metal-poor globular clusters and the intra-cluster light (Durrell et al 2014), suggesting a common origin for these two structures. The deep imaging by Duc et al (2015) revealed a large number of features surrounding their galaxies. Both these projects targeted mostly early-type galaxies. Unfortunately, the pipeline used for the reduction of the Wide Synoptic CFHT Legacy Survey removed the low

surface brightness features around the brightest extended galaxies in the images, producing obvious “holes” that prevent the use of this reduced dataset for the exploration of the outermost parts of the spiral galaxies. In the later MegaCam surveys this problem does not occur.

Another telescope that has revolutionized our understanding of galaxies is the Sloan 2.5 m telescope. The Sloan telescope is well known for producing the SDSS (York et al 2000). Among the different projects that Sloan has covered, of particular interest here is its deep imaging survey in the Southern Galactic cap, popularly known as the “Stripe 82” survey (Jiang et al 2008; Abazajian et al 2009). The Stripe 82 survey covers an area of 275 square degrees along the celestial equator ($-50^\circ < \text{R.A.} < 60^\circ$, $-1.25 < \text{Dec.} < 1.25$) and has been observed in all the five SDSS filters: *ugriz*. The typical amount of time on source was ~ 1.2 h. Being located at the equator, the Stripe 82 area is accessible from most ground-based facilities. A third of all the available SDSS data in the Stripe 82 area were combined by Annis et al (2014). They reached a depth (50% completeness for point sources) of $r \sim 24.2$ mag. Later on, Jiang et al (2014) used the entire dataset and reported a gain of 0.3 – 0.5 mag in depth compared to the previous reduction. None of these reductions were done with the aim of exploring the lowest surface brightness features of the objects. This task was performed by Fliri and Trujillo (2016) and is known as the IAC Stripe 82 Legacy Project. Fliri and Trujillo (2016) reached a depth of $r \sim 24.7$ mag (50% completeness for point sources) and a limiting surface brightness of $\mu_r \sim 28.5$ mag arcsec $^{-2}$ (3σ in 10×10 arcsec 2). The reduced images of Fliri and Trujillo (2016) have been made publicly available through a dedicated webpage (<http://www.iac.es/proyecto/stripe82>).

3.2 *Small Telescopes*

As surface brightness is independent of telescope aperture, in principle one can use small telescopes to reach ultra-faint surface brightness levels. Direct advantages of using small telescopes over larger ones include the larger field of view, and the reduced competition for observing time, in particular when private telescopes are used. Using modern CCD technology, this has been done by several workers in the field, aiming to uncover light sources as diverse as intra-cluster light, diffuse galaxies, or the outer regions of bright galaxies. The Chapter by Abraham et al (this volume) gives significantly more detail on this; we review the basics in this short Section.

Mihos and collaborators used the Case Western Reserve University’s Burrell Schmidt 0.6 m telescope to obtain ultra-deep imaging of the core region of the Virgo cluster, down to limits of $\mu_V = 28.5$ mag arcsec $^{-2}$ (see Mihos et al 2016 for a recent update). From these images, they were able to reveal a number of interesting features of the intra-cluster light, including several tidal streamers of more than 100 kpc in length, and many smaller tidal tails and bridges between galaxies, and to conclude that cluster assembly appears to be hierarchical in nature rather than the product

of smooth accretion around a central galaxy (Mihos et al 2005; the colours of features in the intra-cluster light were measured by Rudick et al 2010). Mihos et al (2015) used the same data set to find three large and extremely low surface brightness galaxies, only one of which shows the signs of tidal damage that might be expected for such galaxies in a dense cluster environment. The same telescope was used by Mihos et al (2013) to image the galaxy M101 over an area of 6 deg^2 and to a depth of $\mu_B = 29.5 \text{ mag arcsec}^{-2}$, and by Watkins et al (2014) to push down to $\mu_B = 30.1 \text{ mag arcsec}^{-2}$ in the M96 galaxy group. The former authors found a number of plumes and spurs but no very extended tidal tails, suggestive of ongoing evolution of the outer disk of the galaxy due to encounters in its group environment, whereas the latter found no optical counterpart to the extended HI surrounding the central elliptical M105, and in general only very subtle interaction signatures in the M96 group.

In a fruitful collaboration with amateur astronomers, Martínez-Delgado et al (2008, 2010, 2015) have used small private telescopes to obtain deep images of tidal streams around a number of galaxies, most with pre-existing evidence for the presence of some kind of outer structure, and more recently of low surface brightness galaxies in the fields of large nearby galaxies (e.g., Javanmardi et al 2016). This group uses very long exposures taken at dark sites, imaging through wide filters. Among the most beautiful and well-known results obtained by Martínez-Delgado's group is the discovery of the optical analogues to the morphologies predicted from N -body models of stellar haloes constructed from satellite accretion (e.g., Bullock and Johnston 2005; Johnston et al 2008). While the resemblance between models and observations is indeed striking and important, it must be kept in mind that most of the structure seen in the models is at lower or much lower surface brightness levels than even the deepest currently available imaging, and that most galaxies observed by Martínez-Delgado et al were targeted specifically to have some previous evidence for tidal structure and are thus not representative of the general galaxy population. In fact, many nearby galaxies show no evidence at all for any tidal or other disturbances in deep images (e.g., Duc et al 2015, see also Merritt et al 2016).

A third strand, besides using small existing research telescopes or amateur installations, is to use simple, small, custom-built telescopes optimized for deep imaging through simple optics and a very careful treatment of systematics. The best-known example of this is the Dragonfly Telephoto Array (Abraham and van Dokkum 2014), a set of up to 48 commercial telephoto lenses with excellent coatings coupled to CCD cameras, which minimizes the amount of scattered light produced inside the telescope. In the current configuration, the array is equivalent to a 1 m aperture telescope with a field of view of 6 square degrees (Abraham and van Dokkum 2014; Abraham 2016; see also Abraham et al, this volume).

Among the results obtained with Dragonfly images and profiles (which go down to $\mu_g \sim 28 \text{ mag arcsec}^{-2}$; 3σ in $12 \times 12 \text{ arcsec}$ boxes; Merritt et al 2016) are the finding that there is a significant spread in the stellar mass fraction surrounding galaxies (van Dokkum et al 2014; Merritt et al 2016, see also Sect. 4.4), and a study of a so-called ultra-diffuse galaxies in the Coma cluster (van Dokkum et al 2016 and references therein).

3.3 Large Telescopes

Large (8-10 m class) telescopes have barely been used so far to obtain very deep imaging of nearby galaxies. To the best of our knowledge the first successful attempt of going ultra-deep (i.e., surpassing the $30 \text{ mag arcsec}^{-2}$ barrier) was conducted by Jablonka et al (2010), who used the imaging mode of the Visible Multi-Object Spectrograph (VIMOS) on ESO's Very Large Telescope (VLT) to target the edge-on S0 galaxy NGC 3957 reaching surface brightness limits (Vega system) of $\mu_R = 30.6 \text{ mag arcsec}^{-2}$ (1σ ; 6 h) and $\mu_V = 31.4 \text{ mag arcsec}^{-2}$ (1σ ; 7 h). These authors found that the stellar halo of this galaxy, calculated between 5 and 8 kpc above the disk plane, is consistent with an old and preferentially metal-poor normal stellar population, like that revealed in nearby galaxy haloes from studies of their resolved stellar content. Also worth mentioning is the work by Galaz et al (2015), who used the more "modest" 6.5 m Magellan telescope to observe the extremely large galaxy Malin 1. Galaz et al (2015) used the Megacam camera to image the galaxy for about 4.5 h in g and r , reaching $\mu_B \sim 28 \text{ mag arcsec}^{-2}$. Using these images, they obtain an impressive result for the diameter of Malin 1 of 160 kpc, ~ 50 kpc larger than previous estimates. Their analysis shows that the observed spiral arms reach very low luminosity and mass surface densities, to levels much lower than the corresponding values for the Milky Way.

The currently deepest ever image of a nearby galaxy was recently obtained by Trujillo and Fliri (2016). These authors pointed the Gran Telescopio Canarias (GTC, a 10.4 m telescope) at the galaxy UGC 00180, an object similar to M31 but located at a distance of ~ 150 Mpc (see Fig. 3). Their r -band image reached a limiting surface brightness of $31.5 \text{ mag arcsec}^{-2}$ (3σ ; $10 \times 10 \text{ arcsec}^2$) after 8.1 h on-source integration. This image revealed a stellar halo with significant structure surrounding the galaxy. The stellar halo has a mass fraction of $\sim 3\%$ of the total stellar mass of the galaxy. This value is close to the one found in the Milky Way and M31 using star counting techniques. This is the first time that integrated-light observations of galaxies reach a surface brightness depth close to that achieved using star counting techniques in nearby galaxies. It is a major step forward as it allows the exploration of the stellar haloes in hundreds of galaxies beyond the Local Group, in particular when viewed in the context of future imaging possibilities with the Large Synoptic Survey Telescope (LSST; see Sect. 5).

4 Disk and Stellar Halo Properties from Ultra-deep Imaging

4.1 Thick Disks

A thick disk is seen as an excess of flux above and below the mid-plane of edge-on and highly inclined galaxies, typically at a few times the scale height of the thin disk component and with a larger exponential scale height than the thin disk

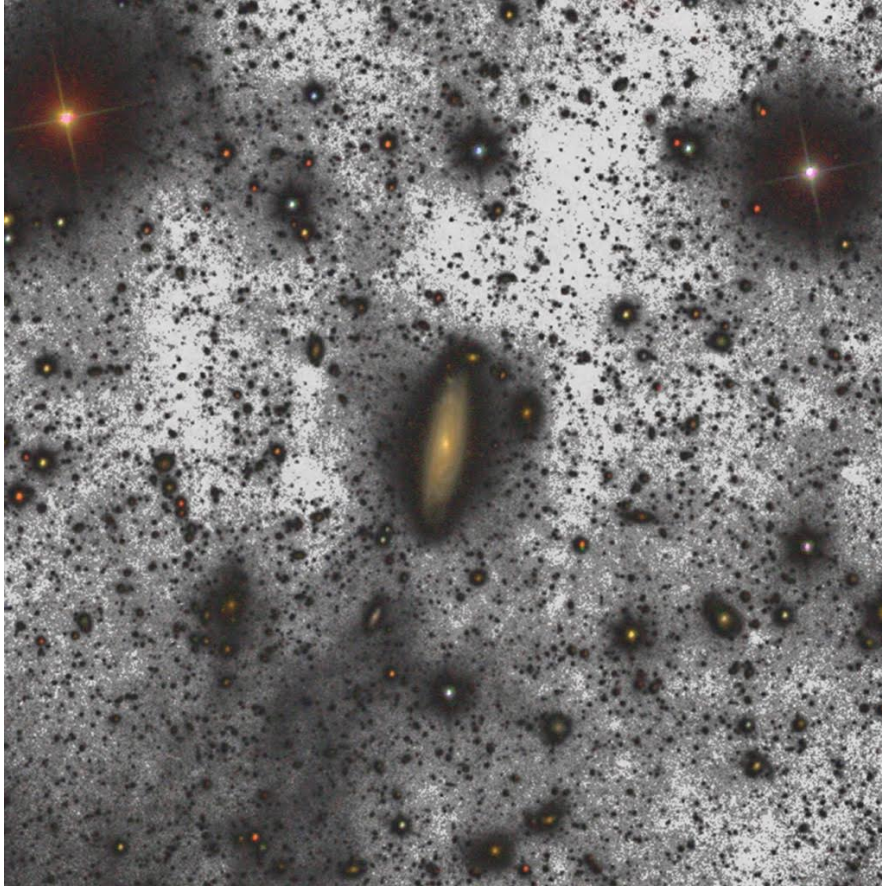


Fig. 3 The galaxy UGC 00180 and its surrounding field observed down to a surface brightness limit of $31.5 \text{ mag arcsec}^{-2}$ in the r -band (around 10 times deeper than most of the previous deep images obtained from the ground). The image is a combination of SDSS imaging (colour part) and 8.1 h of imaging with the GTC; grey part). In addition to the stellar halo of the galaxy, the image shows a plethora of details. Among the most remarkable is the filamentary emission from dust of our own Galaxy located in the bottom-left part of the image. There are also distant galaxies which are seen to be merging with other objects, and a high-redshift cluster towards the bottom-left corner of the galaxy where the intra cluster light is visible. Credit: GTC, Gabriel Pérez and Ignacio Trujillo (IAC)

which is dominant in the mid-plane regions. Thick disks in external galaxies were discovered and defined by Tsikoudi (1979) and Burstein (1979), and have since been found to be very common, in all kinds of galaxies (see, e.g., Dalcanton and Bernstein 2002, Yoachim and Dalcanton 2006, Comerón et al 2011a, Comerón et al 2011b). Our Milky Way has also been known for a long time to have a thick disk component (e.g., Yoshii 1982, Gilmore and Reid 1983), with stars in the thick disk

having significantly lower metallicity than those in the thin component (Gilmore and Wyse 1985).

There is an ongoing debate on the issue of the definition of a thick disk. Early work on the thick disk in the Milky Way, and practically all work on extragalactic thick disks, basically fits stellar density distributions with thin and thick disk components, thus defining them *geometrically*. It is natural to assume that the stars forming part of the thus defined thick component have higher velocity dispersion, and possibly older ages and lower metallicity, than those in the thin disk. In our Milky Way, one can observe individual stars and one can thus define the thick disk *chemically*, for instance by measuring their α -element abundances relative to iron. Some of the interesting consequences of this are the confirmation by Bensby et al (2014) that the scale length of the thick disk is much shorter than that of the thin disk, or even the statement by Bovy et al (2012) that the Milky Way does not have a distinct thick disk at all but rather a continuous distribution of disk thicknesses (but see comments by Haywood et al 2013). This is an ongoing discussion which we note but will not review here. The interested reader may find more discussion and references in a recent conference discussion published by Kawata and Chiappini (2016).

Different formation mechanisms, which can be grouped into three main families, have been proposed for thick disks. All mechanisms directly link the properties of thick disks to the evolution of galaxies, and some indicate clear constraints on the formation of disks. The latter category includes the first broad class of models, in which the high velocity dispersion of the material forming the disk at high redshift led to the thick disk; the thin disk formed later from lower-dispersion material (e.g., Samland and Gerhard 2003; Brook et al 2004; Elmegreen and Elmegreen 2006; Bournaud et al 2009). The second class of models implies a secular origin for thick disks, by stipulating that they are caused by vertical heating and/or the radial migration of stars (e.g., Villumsen 1985; Schönrich and Binney 2009; see also the review by Debattista et al, this volume). In the third class of models the thick disk arises from interactions with satellite galaxies, through the accretion of stars (e.g., Quinn et al 1993) or through dynamical heating (e.g., Abadi et al 2003). No consensus exists as yet in the literature as to which model is the most adequate, and it is likely that all play some role in the formation of thick disks.

Focussing now on the detection and characterisation of extragalactic thick disks, there are two main techniques in use: star counts and direct imaging. The former can be done only in the nearest of external galaxies and only with the *HST*, the latter, in principle, across much larger samples (see below). Older work on resolved stars with *HST* includes that by Mould (2005), Tikhonov and Galazutdinova (2005), Seth et al (2005), and Rejkuba et al (2009), who use resolved red giant branch (RGB) stars to characterize the thick disk component in one or a handful of galaxies. Recent *HST* work includes that by Streich et al (2016) who used images from the GHOSTS survey to note the absence of a separate thick disk component for three of their survey galaxies (although their choice of galaxies was not optimal: they are of low mass, so dust lanes are weak or absent and hence the inclination cannot be

established well—an important point as thick disks are optimally studied in edge-on galaxies).

Among the most comprehensive studies of samples of external galaxies is that by Yoachim and Dalcanton (2006) who used mainly R -band imaging of 34 late-type edge-on disk galaxies to measure the main structural parameters of the thin and thick disk components by fitting one-dimensional analytic expressions based on the generalized function $\text{sech}^{2/n}$. Although such functions give decent fits to profiles, they are essentially *ad hoc* and, in the case of superposed fits of both a thin and a thick disk, ignore the gravitational interaction between the two disk components and therefore are not well justified physically.

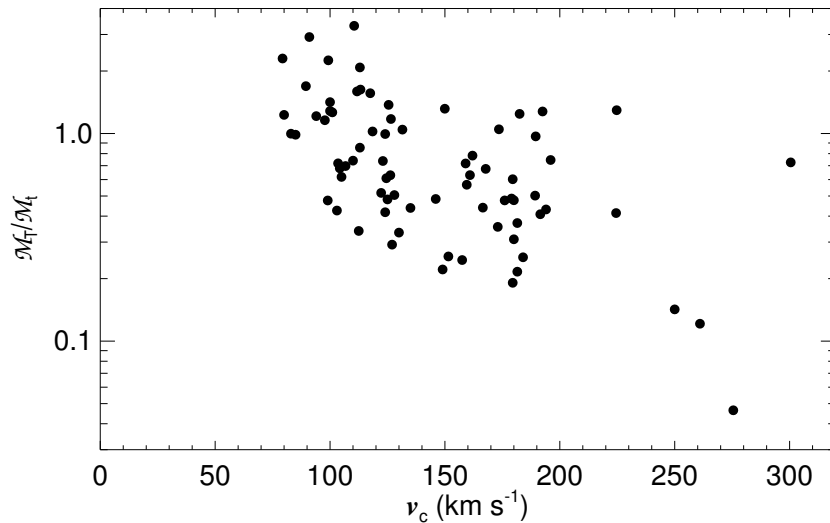


Fig. 4 Ratio of the mass of the thick to that of the thin disk, M_T/M_t , as function of circular velocity v_c for a sample of edge-on galaxies expanded from that of Comerón et al (2012). The new analysis underlying these data incorporates PSF modelling and correction. A value of unity indicates equal thick and thin disk masses. Figure reproduced with permission from S. Comerón et al (in prep.)

To remedy this, Comerón et al (2011a) integrate the equations of equilibrium for a set of gravitationally coupled isothermal stellar and gas disks to derive the parameters of the thin and thick disk components, in particular their relative masses. These authors used deep imaging at $3.6 \mu\text{m}$ from the *Spitzer* Survey of Stellar Structure in Galaxies (S⁴G; Sheth et al 2010), which have the advantage of being essentially unaffected by dust—an important consideration when studying edge-on galaxies. Fitting one-dimensional luminosity profiles obtained from the images of 46 edge-on and highly inclined galaxies, after a careful masking and background-modelling and -subtraction effort, Comerón et al (2011a) found that thick disks are not only ubiquitous, but also significantly more massive than previously reported. Typically, thick and thin disks have comparable masses (Fig. 4), which favours an *in situ* origin

for the thick disk component, with possibly significant additional amounts of stars from satellites that were accreted after the formation of the galaxy, or from secular heating of the thin disk. Because of the different mass-to-light ratios in thin and thick disks, the reported higher mass fractions in the thick component lead to higher overall disk masses, and thus a reduced need for dark matter.

In a later paper, Comerón et al (2012) confirmed this basic result with a somewhat larger sample of 70 edge-on galaxies, while Comerón et al (2014) used an analysis of the thin and thick disk components as well as of the central mass concentrations (CMCs; “bulges”) to conclude that the ratio of the mass of the dynamically hot components (thick disk and CMC) and that of the cold components (thin and gas disks) is constant and does not depend on the mass of the galaxy. This suggests that both the thick disk and the CMC were formed early on, in a short phase of intense star formation activity, and in a turbulent gas disk. The other components were formed later, in a slower phase of lower star formation intensity. Recent work (S. Comerón et al, in prep.) shows that PSF effects in the S⁴G imaging are small enough not to influence any of these main conclusions.

Future work will focus on a number of different areas. Firstly, building larger samples of galaxies with accurately determined thick disk properties, both locally and at higher redshift. The deepest *HST* imaging (e.g., of the *Hubble* ultra-deep fields) can in principle be used for the latter, while the LSST (see Sect. 5) should provide the deep imaging of huge samples of nearby galaxies. Secondly, obtaining detailed information on the kinematics and stellar populations of the thick disks. This is starting to be done now with large telescopes. For instance, Comerón et al (2015) used observations with the VIMOS instrument on ESO’s Very Large Telescope (VLT) to deduce from its kinematics and stellar populations that the thick disk in the galaxy ESO 533-4 formed in a relatively short event, Comerón et al (2016) used MUSE on the VLT to conclude that the thick disk in the S0 galaxy ESO 243-49 formed early on in the history of the galaxy, and before the star formation in the galaxy was quenched, while Kasparova et al (2016) and Guérou et al (2016) provide further evidence that the formation mechanisms of thick disks in galaxies are diverse. Deep spectroscopy with large telescopes, as well as careful colour measurements from LSST imaging, will no doubt bring further progress here, and thus shine light on the formation of disk galaxies.

4.2 Truncations

The relatively sharp edges of edge-on stellar disks, referred to as truncations, were first noted by van der Kruit (1979). Such truncations, typically occurring at radii of around four or five times the exponential scale-length of the inner disk and with scale lengths of less than 1 kpc, appear to be very common, with about three out of four thin discs truncated (Comerón et al 2012, see the review by van der Kruit and Freeman 2011 for further details).

Truncations are important as they are potential key indicators of the formation and early evolution processes that have shaped disk galaxies, as reviewed in detail by van der Kruit and Freeman (2011), in particular in their Sect. 3.8. For instance, as the truncation corresponds to the maximum in the distribution of specific angular momentum across the disk, it may indicate directly what that distribution was in the proto-galaxy, in the case of conservation of angular momentum. Re-distribution of material in the disk, as reviewed by Debattista et al (this volume), may have occurred, leading to the current distribution of angular momentum being unrelated to that of the material that formed the disk. In addition, as reviewed by Elmegreen and Hunter (this volume), disk breaks and truncations are intimately related to the past and present star formation processes in disks.

While it is thus important to characterize truncations, only in edge-on galaxies are they bright enough to have been observed routinely for the past decades, first on the basis of photographic imaging and later using CCDs. Imaging them in face-on or moderately inclined galaxies has so far proven mostly elusive. Not only will truncations occur at much fainter levels there because of reduced line-of-sight integration through the disk, they can also be masked by the lopsided nature of spiral galaxies (e.g., Zaritsky et al 2013), or confused by the onset of stellar haloes (Martín-Navarro et al 2014). In addition, “disk” breaks at relatively high surface brightnesses and occurring at $\sim 8 \pm 1$ kpc in edge-on galaxies have been confused in the literature with truncations, at $\sim 14 \pm 2$ kpc (Martín-Navarro et al 2012). For instance, the features labelled as truncations by Pohlen and Trujillo (2006) most probably are disk breaks rather than the face-on counterparts of the truncations observed in edge-on galaxies.

Using some of the deepest imaging available for samples of nearby galaxies, the SDSS Stripe 82 dataset (see Fliri and Trujillo 2016 and Sect. 3.1), Peters et al (2017) have recently attempted to find the elusive truncations in a sample of 22 face-on to moderately inclined galaxies. They used the new data products from Fliri and Trujillo (2016) and added the g' , r' and i' images to reach extra depth. They selected their galaxies to be undisturbed, and with well-behaved image backgrounds, and were able to extract surface photometry down to $29 - 30 r'$ -mag arcsec $^{-2}$ after performing careful but aggressive masking and modelling of residual background gradients (see Fig. 1 for an example). Peters et al (2017) then used and compared a variety of different analysis and extraction methods to optimize the detection and characterisation of truncations in their sample galaxies.

Figure 5 illustrates many of the results of Peters et al (2017). Firstly, disk breaks at relatively high surface brightness were found in the radial profiles of most galaxies (blue dots in the figure), at levels of typically $22 - 24 r'$ -mag arcsec $^{-2}$. Their radius scales with galaxy radius. Secondly, truncations were indeed identified in three of these moderately inclined galaxies, at surface brightness levels of around $28 r'$ -mag arcsec $^{-2}$. Thirdly, in most galaxies a flattening of the radial profile is seen, interpreted as the onset of the stellar halo², and starting to dominate the profiles at $28 \pm 1 r'$ -mag arcsec $^{-2}$. Fourthly, not only do the radii of the onsets of the truncation and the halo components scale with galaxy size, for some reason they do that in the

² Peters et al (2017) perform a careful PSF modelling to ensure that the observed haloes are not artifacts caused by the PSF.

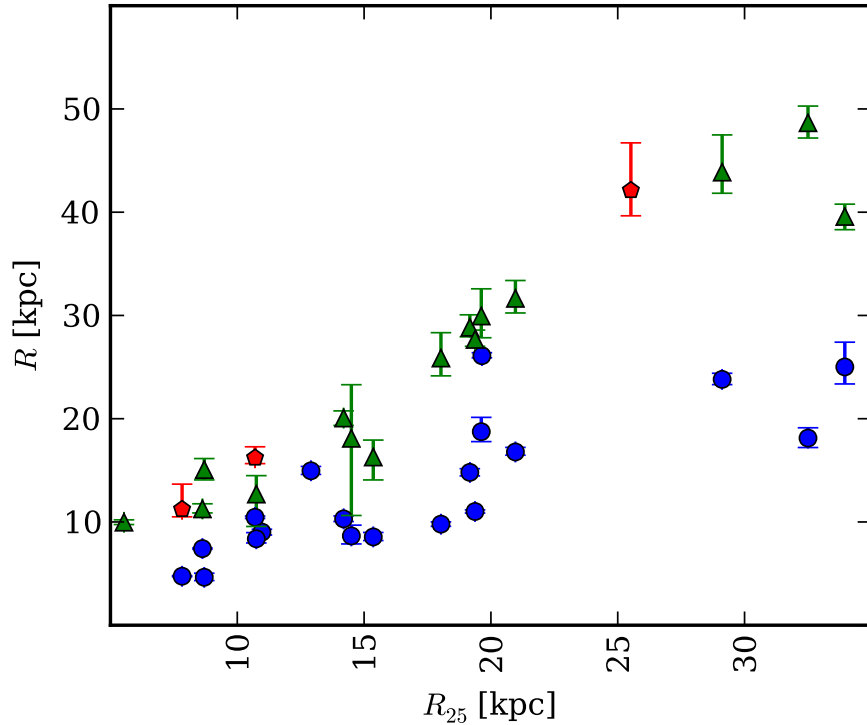


Fig. 5 Feature size R as a function of galaxy size, indicated by R_{25} , for the moderately inclined to face-on galaxies in the sample of Peters et al (2017). Red pentagons represent truncations, green triangles the onset of the stellar halo, and blue circles disk breaks which occur further inside the disk. Reproduced with permission from Peters et al (2017)

same manner, so that truncation and halo points (red pentagons and green triangles, respectively, in Fig. 5) line up on the same relation. This intriguing relation deserves further attention with other independent surveys, as these features are barely above the surface brightness limit of the Stripe82.

A further very interesting observation from Peters et al (2017) is that truncations are only observed in those galaxies from which the halo component is either absent or fainter than usual, although no indications were found from galaxy or feature parameters as to why the halo might be faint or absent. Of the seven galaxies with faint or absent haloes, three were found to host truncations. This is not out of line with the statistical result of Kregel et al (2002) that at least 20 of their 34 edge-on galaxies were truncated. More detailed study of larger samples of galaxies should shed further light on these important issues, and future developments are promising in this respect (see Sect. 5).

4.3 Tidal Streams

Tidal streams are the imprints of the ongoing merging activity of galaxies. They are present around a significant fraction of galaxies, showing different shapes, brightnesses and extensions depending on their progenitor's mass and orbit. The structural (and kinematical) properties of tidal streams can be used to infer information about the dark matter haloes in which the host galaxies are embedded (Bullock and Johnston 2005). These authors conclude that the vast majority of stream features have very low surface brightness ($\mu_V \gtrsim 28.5 \text{ mag arcsec}^{-2}$). More precisely, cosmological simulations predict around one detectable stream per galaxy if the observations reach a depth of $\sim 30 \text{ mag arcsec}^{-2}$ (e.g., Bullock and Johnston 2005; Johnston et al 2008; Cooper et al 2010). This makes the use of very deep surveys mandatory if one wants to have a complete census of past merging activity.

The detailed analysis of our Milky Way and the Andromeda galaxy M31 (using the star count technique) has revealed a plethora of substructure in these objects. Due to the vicinity of these galaxies, the star count technique can reveal features which have surface brightnesses equivalent to $\mu_V \sim 32 \text{ mag arcsec}^{-2}$ (e.g., Ibata et al 2001; Majewski et al 2003; Belokurov et al 2006; Bell et al 2008; McConnachie et al 2009). These levels are extremely challenging to reach using integrated photometry (the only case published to date is that of the galaxy explored in Trujillo and Fliri 2016). The need, however, for conducting an extensive survey exploring the variety of features around galaxies like the Milky Way is pressing. In fact, according to theory, a large galaxy-to-galaxy variation is expected due to the intrinsic stochasticity of the merger phenomenon. For this reason, to have a proper comparison with theory it is urgent to have a large survey exploring hundreds of galaxies beyond the Local Group. This is only achievable using the integrated photometry technique. The star count technique becomes unfeasible (with current telescopes) beyond $\sim 16 \text{ Mpc}$ (Zackrisson et al 2012).

The first attempt to systematize the search for streams in galaxies beyond the Local Group has been made by Martínez-Delgado et al (2010). These authors use modest ($\lesssim 1 \text{ m}$) aperture telescopes using integration times $\sim 10\text{-}20 \text{ h}$, allowing them to reach $\mu_g \sim 28.5 \text{ mag/arcsec}^2$. They have found a large variety of tidal stream morphologies in eight nearby galaxies: large arc-like features, giant “umbrellas”, shells, plumes, spiral-like patterns, etc. These morphologies are similar, at least qualitatively, to those expected in cosmological simulations. However, the galaxies explored in Martínez-Delgado et al (2010) are not representative of the general galaxy population as they were preselected to have bright structure surrounding them. In this sense, despite the effort of these authors, the comparison of theory with observations remains currently in its infancy. This is because a large survey, probing hundreds of randomly selected galaxies, is still missing.

4.4 *Stellar Haloes*

Tidal streams and stellar haloes around galaxies are intimately connected. In fact, in observations with enough resolution and signal-to-noise stellar haloes should appear as a combination of many different merger events (and consequently, the sum of many tidal streams). Stellar haloes also have a diffuse component which corresponds to those accretion events that happened very early on in a galaxy's evolution. Whereas bright tidal streams inform us about the ongoing or recent merging activity of a galaxy, stellar haloes give us information about the past accretion story of galaxies.

In contrast with numerical simulations, where the characterization of the stellar halo is relatively simple, there is no agreement in the literature on how to quantify the properties of stellar haloes using images of galaxies alone. Simulations (e.g., Cooper et al 2010; Font et al 2011; Tissera et al 2014; Pillepich et al 2014) show unequivocally that the contribution of accreted stars rises towards the centre of galaxies. In fact, in numerical simulations the accreted material follows surface mass distributions that can be modelled well with Sérsic (with Sérsic indexes $n \lesssim 3$) or power-law profiles (with logarithmic slope ~ 3.5) for the 3D density profiles. Accreted stars are the main contributors to the stellar mass surface distribution of galaxies in their outer regions, however, towards the inner zones they contribute much less in comparison with the stars that have formed *in situ* (a factor of ~ 100 in projected density; Cooper et al 2013).

The observational characterization of stellar halo profiles has followed different approaches. Several authors fit the outer (stellar halo-dominated) surface brightness region with some analytical profile, for instance, exponential (e.g., Irwin et al 2005; Ibata et al 2007; Trujillo and Fliri 2016) or power-law (with logarithmic slopes ~ 2.5 ; e.g., Tanaka et al 2010; Courteau et al 2011; Gilbert et al 2012). This approach has the disadvantage of assuming a particular shape of the stellar halo towards the inner region of galaxies, motivated by numerical simulations. This shape is derived by extrapolating the fit to the outer region towards the inner area. There is no way of eliminating this assumption observationally with integrated photometry alone, because in the central part of the galaxy the light is dominated by the bulge and disk. Other authors avoid making any assumption about the inner shape of the stellar halo profile and measure the properties of the stellar halo only in the outer regions where the halo is the dominant contribution. For instance, Buitrago et al (2016), for elliptical galaxies, use the radial region $10 < R(\text{kpc}) < 50$ whereas Merritt et al (2016) use $R(\text{kpc}) > 5R_h$ (with R_h the half-mass radius) for spiral galaxies. This approach has the disadvantage of neglecting the (dominant) contribution of the stellar light of the halo in the innermost region of the galaxy. Any of the two above approaches to measure the relevance of the stellar halo can be followed if a proper comparison (i.e., following the same scheme) is conducted with the numerically simulated galaxies as well. In the literature it is common to find a comparison of the amount of stellar mass in the stellar halo with the total stellar mass of the galaxy. This relation is then compared with numerical predictions (see, e.g., Fig. 6). Observers directly measure neither the light contribution from the stellar haloes nor the stellar mass. To

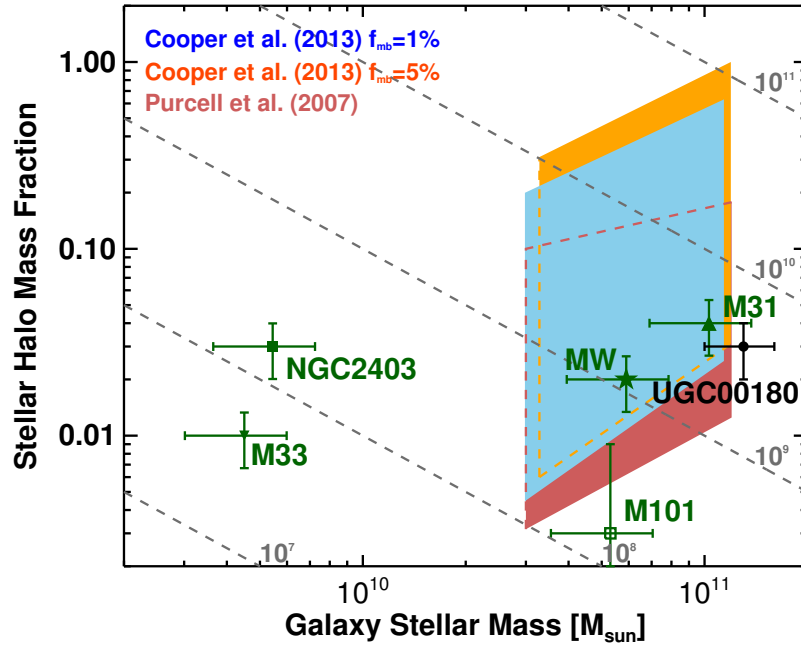


Fig. 6 Stellar halo mass fraction versus total galaxy stellar mass, illustrating the location of some nearby galaxies in this plane. In addition, the prediction from several numerical models are over-plotted (Purcell et al 2007; Cooper et al 2013). The dashed lines are the locations of stellar haloes with fixed stellar mass (10^7 , 10^8 , 10^9 , 10^{10} and $10^{11} M_{\odot}$). Figure from Trujillo and Fliri (2016), reproduced by permission of the AAS

transform from light to stellar mass it is necessary to estimate a stellar mass to light ratio. This can be done using photometric information from several filters (when available).

The fraction of mass in the stellar haloes of disk (Milky Way-like) galaxies is around 1%. However, there are notable exceptions like M101, which does not show evidence for a stellar halo (van Dokkum et al 2014) even when using deep imaging. Observed stellar haloes are, in general, less massive than expected from theory. Nonetheless, the number of observed galaxies is still too limited to consider this as a serious concern.

Measuring the amount of stellar mass in the stellar halo is a strong test to probe the predictions from the Λ -Cold Dark Matter (ACDM) model in the context of galaxy formation. Ultimately, the amount of stars in this component of the galaxy informs us about the merging activity along the full history of the galaxy. Consequently, if the observed stellar haloes are less massive than the theoretical expectations this might indicate that the number of accretion events was less than

presumed. If this were in fact the case, we could be witnessing a problem for the Λ CDM scheme as relevant as the missing satellite problem (see Sect. 4.5).

4.4.1 PSF Effects on Imaging the Outermost Regions of Galaxies

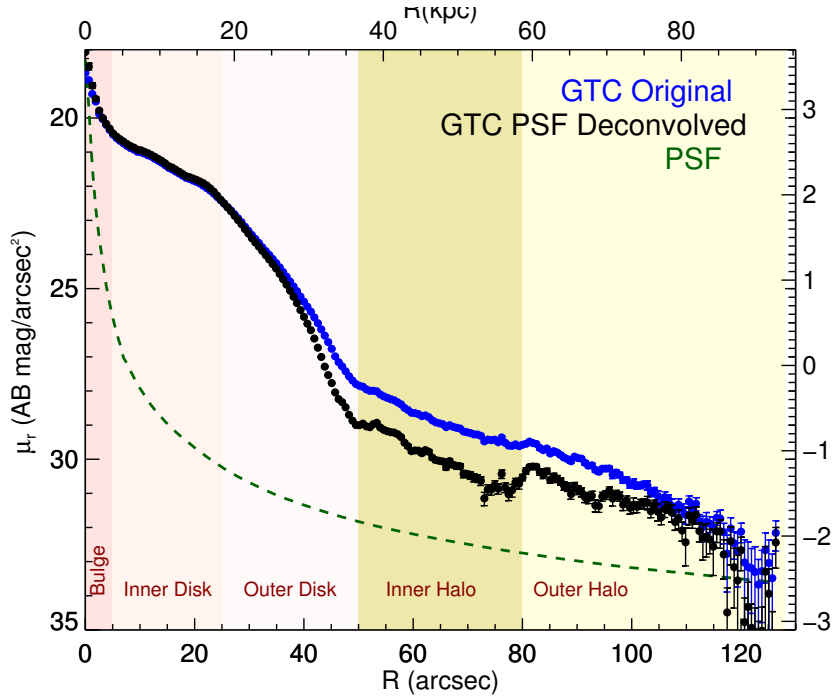


Fig. 7 The effect of the PSF on the surface brightness profile of the spiral galaxy UGC 00180. The observed profile (upper one) is shown using blue dots. The profile corrected for the effect of the PSF (lower profile) is illustrated with black dots. The green dashed line is the surface brightness profile of the PSF of the image. The different parts of the galaxy are indicated with labels. Figure from Trujillo and Fliri (2016), reproduced by permission of the AAS

As discussed in Sect. 2.5, one of the most important sources of light contamination in deep images is the contribution of scattered light from nearby sources surrounding the target galaxy. However, the galaxy itself is usually one of the most important sources of light contamination in the vicinity of the object. This is easy to understand. The surface brightness distribution of the galaxy is convolved with the PSF of the image. That means that a substantial amount of light coming from the central parts of the galaxy is distributed into its outermost region. Sandin (2014, 2015) has nicely illustrated this phenomenon, showing that the scattered light from the object (if not accounted for) can be wrongly interpreted as a bright stellar halo

or a thick disk. This was also explored by de Jong (2008). Depending on the shape of the surface brightness distribution of the galaxy, the effect of its own scattered light can be more or less relevant in its outer region. Edge-on disks are normally most severely affected by this effect, whereas face-on galaxies without breaks or truncations are barely affected. As a general rule, the effect will be stronger in those cases where the light distribution is sharper. In Fig. 7, we show an example of the effect of the PSF on the light distribution of a spiral galaxy.

As Fig. 7 illustrates, the effect of the PSF on the outer regions of the galaxy is dramatic. For this particular galaxy, the surface brightness profiles start to deviate at around $26 \text{ mag arcsec}^{-2}$. At $\mu_r \sim 26 \text{ mag arcsec}^{-2}$, the effect is so important that the surface brightness profiles (affected by the PSF and corrected) are different by about 1 mag. This means that in the outer regions the scattered light can be as much as three times brighter than the intrinsic light of the stellar halo. For this reason, it is absolutely necessary to model the effect of the PSF on the galaxy itself if one wants to explore the faintest regions of the galaxies.

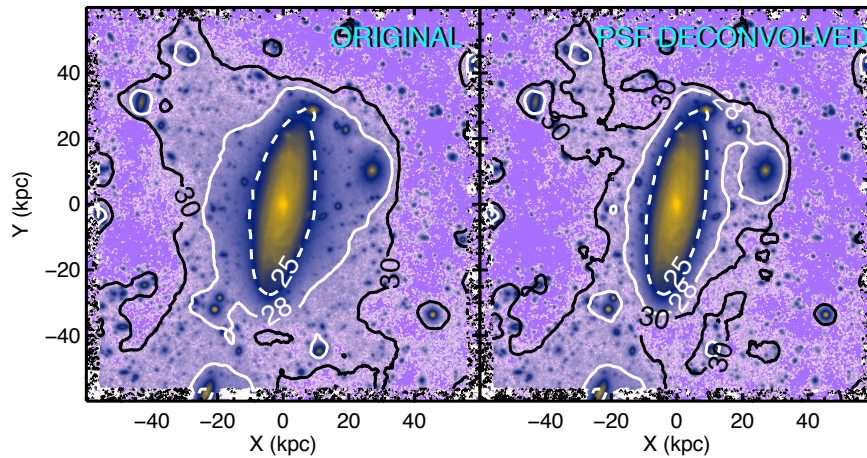


Fig. 8 The dramatic effect of the PSF on the surface brightness distribution of the spiral galaxy UGC 00180. Different surface brightness isophotes are indicated with solid and dashed lines. After accounting for the effect of the PSF the amount of light in the outer regions decreases strongly. Figure from Trujillo and Fliri (2016), reproduced by permission of the AAS

There are two different approaches to handle the effect of the PSF on the surface brightness distribution of the galaxies. The first one is to apply a deconvolution method directly on the images. This has the advantage that it only requires an exquisitely characterized PSF of the image. However, its main disadvantage is that in the regions where the surface brightness is closest to the noise the result is quite uncertain. The second approach is to model the intrinsic light distribution of the galaxy and convolve this with the PSF. The convolved model of the galaxy is then fitted to the observed light distribution until a good fit to the data is reached. Once

this is achieved, a new image of the object (using the deconvolved model of the galaxy) is created, adding back the residuals of the fit. This is illustrated in Fig. 8.

Figure 8 shows that studies of both thick disks and outer stellar haloes are strongly affected by the PSF. Any deep imaging study of these components needs to account for this effect, otherwise both the stellar haloes and the thick disks that will be inferred will result significantly brighter than what they really are.

4.5 Satellites

Satellites are probably one of the most important pieces to connect the realm of observed galaxies with cosmological modelling. In fact, counting the number of satellites and exploring their properties has become one of the most important tests to explore the predictions of the Λ CDM model on small (i.e., galactic) scales. The analysis of Local Group galaxies has revealed a number of problems related with satellite galaxies. These can be summarized as follows:

- The “missing satellites” problem. Cosmological simulations, in the framework of the Λ CDM model and based only on dark matter particles (i.e., without including the effect of baryons), predict thousands of small dark matter haloes orbiting galaxies like the Milky Way or Andromeda (e.g., Klypin et al 1999; Moore et al 1999). However, only a few tens of visible satellites have been observed around these objects (McConnachie 2012).
- The “too big to fail” problem. In the Λ CDM model, the largest satellite galaxies are expected to have a velocity dispersion substantially larger than what is actually measured in any of the dwarf galaxies in the Local Group (Read et al 2006; Boylan-Kolchin et al 2011). These big haloes among the satellite population should not have failed to produce dwarf galaxies following the prescription of baryonic physics, so if they exist, dwarf galaxies with such large central velocity dispersion should have been found observationally.

There are a number of solutions to the above cosmological problems at galactic scales. One possibility is that the main constituent of dark matter would not be a heavy (i.e., cold) particle but instead a lighter (i.e., warm) candidate (with a mass of around a keV). This hypothesis has been explored in many papers as it is able to suppress many of the dark matter haloes which should form dwarf galaxies (e.g., Moore et al 1999; Bode et al 2001; Avila-Reese et al 2001). This alleviates the problem of the missing satellites. This solution is not free of other problems, however, mainly the current constraint on the mass of the warm dark matter candidate imposed by the study of the Lyman α forest (i.e., $\gtrsim 4$ keV; Baur et al 2016). This mass is large enough to mimic most of the properties of the Λ CDM scenario (including the production of a large number of dark matter subhaloes). Consequently, warm dark matter particle candidates with such minimum mass would not be of great help. Another alternative is to consider the baryon physics in detail when creating realistic cosmological simulations. It is worth stressing that the above problems arise when

comparing simulations of dark matter alone (i.e., devoid of gas and stars) with the frequency and properties of satellites in the Local Group. However, some authors, like Navarro et al (1996) or Read and Gilmore (2005) have pointed out the interplay between baryons and dark matter. In fact, they have suggested that the dark matter could be heated by impulsive gas mass loss driven by supernova explosions. If so, this could help to reconcile the cosmological simulations with the observations.

The above discrepancies between theory and observations are based on the comparison of the properties of the satellite galaxies of two massive disks, i.e., those of our own Galaxy and Andromeda. Consequently, a natural question arises: is our Local Group anomalous in producing a low number of satellites? To address this question in detail, we need to characterize the satellite population of many galaxies like ours beyond the Local Group. This idea has been pursued by several authors (see, e.g., Liu et al 2011; Ruiz et al 2015). Unfortunately, their analyses have only explored the population of the most massive satellites (i.e., down to masses $\sim 10^8 - 10^9 M_\odot$). To test the discrepancies between the cosmological models and the observations it is necessary to go at least two orders of magnitudes fainter (i.e., down to $10^6 M_\odot$). This is where new ultra-deep imaging surveys can play a definitive role (see, e.g., Javanmardi et al 2016). To explore satellites with masses around $10^6 M_\odot$ within a sphere of radius ~ 100 Mpc, we need to be able to reach a depth like the one achieved by Stripe 82. If we want to go further and explore a population of satellites with masses of a few times $10^4 M_\odot$ (which is currently the mass limit of detected satellites in Andromeda) we would need a survey with the depth reached by the current deepest dataset (i.e., the one of Trujillo and Fliri 2016). A survey with such characteristics could be obtained at the end of the LSST programme (Ivezic et al 2008; see Sect. 5).

5 Conclusions and Future Developments

In this Chapter, we have reviewed how deep imaging is a fundamental tool in the study of the outermost structure of galaxies. Three main sources of imaging are currently used to detect and characterize the outskirts of galaxies: (1) surveys such as the Sloan Digital Sky Survey's Stripe 82 project, (2) very long exposures on small telescopes, including by amateurs, and (3) long exposures on the largest professional telescopes. The technical challenges in overcoming systematic effects are significant, and range from the treatment of light scattered by the atmosphere and the telescope and instrument, via flat fielding, to the accurate subtraction of non-galaxy light in the images. We have reviewed recent results on galaxy disks and haloes obtained with deep imaging, including the detection and characterization of thick disks, truncations of stellar disks, tidal streams, stellar haloes, and satellites. We have shown how each of these interrelated aspects of the faintest detectable structure in galaxies can shed light on the formation and subsequent evolution of the galaxies and our Universe.

The future is promising in terms of discovering the “low surface brightness Universe” through deep imaging. Current techniques using small and large ground-based telescopes, as reviewed in Sect. 3, will continue to be exploited while new facilities will become available. The most promising of these new facilities are poised to be the ground-based LSST, and the new space telescopes *JWST* and *Euclid*. LSST (Ivezic et al 2008) will repeatedly image the whole of the Southern sky in 6 passbands (*ugrizy*), with a planned start date for surveys of around 2021. While each 30 s exposure with the 8.2 m telescope and optimized camera will yield a depth of 24.7 *r*-mag (5-sigma point source depth) over the 9.6 square degree field of view, combining all imaging obtained over the approximately 10 year survey duration could yield a depth of 27.5 *r*-mag (5-sigma point source depth). This roughly means as deep as the current Stripe 82 in one exposure, and close to three magnitudes deeper over the whole survey duration. The scientific possibilities offered by this depth of imaging, over an area of sky of over 20000 deg², are tremendous. All the science discussed in this paper could essentially be done with one or a few exposures, or easily with the data of say one hour of observation. This obviously depends critically on whether systematic effects, including but not limited to those discussed in Sect. 2, can be properly controlled, modelled, and corrected for. This is not trivial, and may hinder the full exploitation of the data to their theoretical limits.

The *JWST*, to be launched in 2018, will allow deep imaging but, when compared to, e.g., the *HST*, won't be quite as revolutionary as LSST. The field of view will be limited to just over 2×4 arcmin² in the near-IR which will all but exclude deep imaging of the nearest galaxies. Where significant progress can be expected is in the deep imaging of galaxies at redshifts of, say, 0.2 and higher. In particular, near-IR imaging will allow the observation of galaxies at redshifts beyond 1 in rest-frame red passbands, necessary to reduce the effects of both young stellar populations and dust extinction.

Euclid will provide, among other data products, imaging in a very wide optical band ($R + I + Z$) over an area of 15000 deg² to a depth of 24.5 mag (10σ for extended source). Compared to LSST, advantages of *Euclid* imaging will be its higher spatial resolution (of ~ 0.2 arcsec, due to the relatively small telescope aperture of 1.2 m) and better-behaved PSF, thanks to the absence of the Earth atmosphere. A disadvantage is that the visual imaging is done through a very wide filter which excludes the use of colour information. The depth of imaging will be comparable with LSST, though, for *Euclid's* Deep Survey (over an area of around 40 square degree), which will allow the comparison of high-resolution *Euclid* imaging with the colour information obtained from the LSST images.

The area of ultra-deep imaging is still very much unexplored territory, and future work in this area will be stimulated by the availability of revolutionary new data sets and the continued understanding of the systematics affecting them. It will be a huge technical challenge to properly treat and analyze the upcoming deep imaging, in particular those from LSST and *Euclid*. As we enter previously unexplored territory with ultra-deep imaging, the systematic effects we know about will be challenging to characterize and correct for, and additional difficulties will almost certainly present themselves. But overcoming these issues will definitely pay off in terms of

increased understanding of the formation and evolution processes which have led to the Universe and the galaxies as we observe them now. The future of imaging ultra-faint structures is very bright.

Acknowledgements JHK thanks Sébastien Comerón and Carme Gallart for comments on sections of the manuscript. IT has benefitted from multiple conversations with and the hard work of many members of his team. In particular, he thanks Jürgen Fliri, María Cebrián and Javier Román. JHK and IT acknowledge financial support from the Spanish Ministry of Economy and Competitiveness (MINECO) under grants number AYA2013-41243-P and AYA2013-48226-C3-1-P, respectively. JHK acknowledges financial support to the DAGAL network from the People Programme (Marie Curie Actions) of the European Unions Seventh Framework Programme FP7/2007-2013/ under REA grant agreement number PITN-GA-2011-289313.

References

- Abadi MG, Navarro JF, Steinmetz M, Eke VR (2003) Simulations of Galaxy Formation in a Cold Dark Matter Universe. II. The Fine Structure of Simulated Galactic Disks. *ApJ* 597:21–34, DOI 10.1086/378316, [astro-ph/0212282](#)
- Abazajian KN, Adelman-McCarthy JK, Agüeros MA, Allam SS, Allende Prieto C, An D, Anderson KSJ, Anderson SF, Annis J, Bahcall NA, et al (2009) The Seventh Data Release of the Sloan Digital Sky Survey. *ApJS* 182:543-558, DOI 10.1088/0067-0049/182/2/543, [0812.0649](#)
- Abraham RG (2016) Probing galactic outskirts with Dragonfly. In: Gil de Paz A, Knapen JH, Lee JC (eds) Formation and Evolution of Galaxy Outskirts, CUP, in press, Proc. IAU, CUP, in press
- Abraham RG, van Dokkum PG (2014) Ultra-Low Surface Brightness Imaging with the Dragonfly Telephoto Array. *PASP* 126:55–69, DOI 10.1086/674875, [1401.5473](#)
- Annis J, Soares-Santos M, Strauss MA, Becker AC, Dodelson S, Fan X, Gunn JE, Hao J, Ivezić Ž, Jester S, Jiang L, Johnston DE, Kubo JM, Lampeitl H, Lin H, Lupton RH, Miknaitis G, Seo HJ, Simet M, Yanny B (2014) The Sloan Digital Sky Survey Coadd: 275 deg² of Deep Sloan Digital Sky Survey Imaging on Stripe 82. *ApJ* 794:120, DOI 10.1088/0004-637X/794/2/120, [1111.6619](#)
- Avila-Reese V, Colín P, Valenzuela O, D’Onghia E, Firmani C (2001) Formation and Structure of Halos in a Warm Dark Matter Cosmology. *ApJ* 559:516–530, DOI 10.1086/322411, [astro-ph/0010525](#)
- Baur J, Palanque-Delabrouille N, Yèche C, Magneville C, Viel M (2016) Lyman-alpha forests cool warm dark matter. *JCAP* 8:012, DOI 10.1088/1475-7516/2016/08/012, [1512.01981](#)
- Bell EF, Zucker DB, Belokurov V, Sharma S, Johnston KV, Bullock JS, Hogg DW, Jahnke K, de Jong JTA, Beers TC, Evans NW, Grebel EK, Ivezić Ž, Koposov SE, Rix HW, Schneider DP, Steinmetz M, Zolotov A (2008) The Accretion Origin of the Milky Way’s Stellar Halo. *ApJ* 680:295-311, DOI 10.1086/588032, [0706.0004](#)
- Belokurov V, Zucker DB, Evans NW, Gilmore G, Vidrih S, Bramich DM, Newberg HJ, Wyse RFG, Irwin MJ, Fellhauer M, Hewett PC, Walton NA, Wilkinson MI, Cole N, Yanny B, Rockosi CM, Beers TC, Bell EF, Brinkmann J, Ivezić Ž, Lupton R (2006) The Field of Streams: Sagittarius and Its Siblings. *ApJ* 642:L137–L140, DOI 10.1086/504797, [astro-ph/0605025](#)
- Bensby T, Feltzing S, Oey MS (2014) Exploring the Milky Way stellar disk. A detailed elemental abundance study of 714 F and G dwarf stars in the solar neighbourhood. *A&A* 562:A71, DOI 10.1051/0004-6361/201322631, [1309.2631](#)
- Bertin E, Arnouts S (1996) SExtractor: Software for source extraction. *A&A* 117:393–404, DOI 10.1051/aas:1996164
- Bode P, Ostriker JP, Turok N (2001) Halo Formation in Warm Dark Matter Models. *ApJ* 556:93–107, DOI 10.1086/321541, [astro-ph/0010389](#)

- Bournaud F, Elmegreen BG, Martig M (2009) The Thick Disks of Spiral Galaxies as Relics from Gas-rich, Turbulent, Clumpy Disks at High Redshift. *ApJL*707:L1–L5, DOI 10.1088/0004-637X/707/1/L1, 0910.3677
- Bovy J, Rix HW, Hogg DW (2012) The Milky Way Has No Distinct Thick Disk. *ApJ*751:131, DOI 10.1088/0004-637X/751/2/131, 1111.6585
- Boylan-Kolchin M, Bullock JS, Kaplinghat M (2011) Too big to fail? The puzzling darkness of massive Milky Way subhaloes. *MNRAS* 415:L40–L44, DOI 10.1111/j.1745-3933.2011.01074.x, 1103.0007
- Brook CB, Kawata D, Gibson BK, Freeman KC (2004) The Emergence of the Thick Disk in a Cold Dark Matter Universe. *ApJ*612:894–899, DOI 10.1086/422709, astro-ph/0405306
- Buitrago F, Trujillo I, Curtis-Lake E, Cooper AP, Bruce VA, Montes M, Perez-Gonzalez PG, Cirasuolo M (2016) The cosmic assembly of stellar haloes in massive Early-Type Galaxies. *ArXiv e-prints* 1602.01846
- Bullock JS, Johnston KV (2005) Tracing Galaxy Formation with Stellar Halos. I. Methods. *ApJ* 635:931–949, DOI 10.1086/497422, astro-ph/0506467
- Burstein D (1979) Structure and origin of S0 galaxies. III - The luminosity distribution perpendicular to the plane of the disks in S0's. *ApJ*234:829–836, DOI 10.1086/157563
- Cappellari M, Emsellem E, Krajnović D, McDermid RM, Scott N, Verdoes Kleijn GA, Young LM, Alatalo K, Bacon R, Blitz L, Bois M, Bournaud F, Bureau M, Davies RL, Davis TA, de Zeeuw PT, Duc PA, Khochfar S, Kuntschner H, Lablanche PY, Morganti R, Naab T, Oosterloo T, Sarzi M, Serra P, Weijmans AM (2011) The ATLAS^{3D} project - I. A volume-limited sample of 260 nearby early-type galaxies: science goals and selection criteria. *MNRAS* 413:813–836, DOI 10.1111/j.1365-2966.2010.18174.x, 1012.1551
- Comerón S, Elmegreen BG, Knapen JH, Salo H, Laurikainen E, Laine J, Athanassoula E, Bosma A, Sheth K, Regan MW, Hinz JL, Gil de Paz A, Menéndez-Delmestre K, Mizusawa T, Muñoz-Mateos JC, Seibert M, Kim T, Elmegreen DM, Gadotti DA, Ho LC, Holwerda BW, Lappalainen J, Schinnerer E, Skibba R (2011a) Thick Disks of Edge-on Galaxies Seen through the Spitzer Survey of Stellar Structure in Galaxies (S⁴G): Lair of Missing Baryons? *ApJ*741:28, DOI 10.1088/0004-637X/741/1/28, 1108.0037
- Comerón S, Elmegreen BG, Knapen JH, Sheth K, Hinz JL, Regan MW, Gil de Paz A, Muñoz-Mateos JC, Menéndez-Delmestre K, Seibert M, Kim T, Mizusawa T, Laurikainen E, Salo H, Laine J, Athanassoula E, Bosma A, Buta RJ, Gadotti DA, Ho LC, Holwerda B, Schinnerer E, Zaritsky D (2011b) The Unusual Vertical Mass Distribution of NGC 4013 Seen through the Spitzer Survey of Stellar Structure in Galaxies (S⁴G). *ApJL*738:L17, DOI 10.1088/2041-8205/738/2/L17, 1107.0529
- Comerón S, Elmegreen BG, Salo H, Laurikainen E, Athanassoula E, Bosma A, Knapen JH, Gadotti DA, Sheth K, Hinz JL, Regan MW, Gil de Paz A, Muñoz-Mateos JC, Menéndez-Delmestre K, Seibert M, Kim T, Mizusawa T, Laine J, Ho LC, Holwerda B (2012) Breaks in Thin and Thick Disks of Edge-on Galaxies Imaged in the Spitzer Survey Stellar Structure in Galaxies (S⁴G). *ApJ*759:98, DOI 10.1088/0004-637X/759/2/98, 1209.1513
- Comerón S, Elmegreen BG, Salo H, Laurikainen E, Holwerda BW, Knapen JH (2014) Evidence for the concurrent growth of thick discs and central mass concentrations from S⁴G imaging. *A&A*571:A58, DOI 10.1051/0004-6361/201424412, 1409.0466
- Comerón S, Salo H, Janz J, Laurikainen E, Yoachim P (2015) Galactic archaeology of a thick disc: Excavating ESO 533-4 with VIMOS. *A&A*584:A34, DOI 10.1051/0004-6361/201526815, 1509.03841
- Comerón S, Salo H, Peletier RF, Mentz J (2016) A monolithic collapse origin for the thin and thick disc structure of the S0 galaxy ESO 243-49. *A&A*593:L6, DOI 10.1051/0004-6361/201629292, 1608.04238
- Cooper AP, Cole S, Frenk CS, White SDM, Helly J, Benson AJ, De Lucia G, Helmi A, Jenkins A, Navarro JF, Springel V, Wang J (2010) Galactic stellar haloes in the CDM model. *MNRAS* 406:744–766, DOI 10.1111/j.1365-2966.2010.16740.x, 0910.3211

- Cooper AP, D'Souza R, Kauffmann G, Wang J, Boylan-Kolchin M, Guo Q, Frenk CS, White SDM (2013) Galactic accretion and the outer structure of galaxies in the CDM model. *MNRAS* 434:3348–3367, DOI 10.1093/mnras/stt1245, 1303.6283
- Courteau S, Widrow LM, McDonald M, Guhathakurta P, Gilbert KM, Zhu Y, Beaton RL, Majewski SR (2011) The Luminosity Profile and Structural Parameters of the Andromeda Galaxy. *ApJ* 739:20, DOI 10.1088/0004-637X/739/1/20, 1106.3564
- Cuillandre JCJ, Withington K, Hudelot P, Goranova Y, McCracken H, Magnard F, Mellier Y, Regnault N, Bétoule M, Aussel H, Kavelaars JJ, Fernique P, Bonnarel F, Ochsenbein F, Ilbert O (2012) Introduction to the CFHT Legacy Survey final release (CFHTLS T0007). In: *Observatory Operations: Strategies, Processes, and Systems IV, Proceedings of SPIE*, vol 8448, p 84480M, DOI 10.1117/12.925584
- Dalcanton JJ, Bernstein RA (2002) A Structural and Dynamical Study of Late-Type, Edge-on Galaxies. II. Vertical Color Gradients and the Detection of Ubiquitous Thick Disks. *AJ* 124:1328–1359, DOI 10.1086/342286, astro-ph/0207221
- Dalcanton JJ, Williams BF, Seth AC, Dolphin A, Holtzman J, Rosema K, Skillman ED, Cole A, Girardi L, Gogarten SM, Karachentsev ID, Olsen K, Weisz D, Christensen C, Freeman K, Gilbert K, Gallart C, Harris J, Hodge P, de Jong RS, Karachentseva V, Mateo M, Stetson PB, Tavarez M, Zaritsky D, Governato F, Quinn T (2009) The ACS Nearby Galaxy Survey Treasury. *ApJS* 183:67–108, DOI 10.1088/0067-0049/183/1/67, 0905.3737
- Davies JI, Wilson CD, Auld R, Baes M, Barlow MJ, Bendo GJ, Bock JJ, Boselli A, Bradford M, Buat V, Castro-Rodriguez N, Chaniel P, Charlot S, Ciesla L, Clements DL, Cooray A, Cormier D, Cortese L, Dwek E, Eales SA, Elbaz D, Galametz M, Galliano F, Gear WK, Glenn J, Gomez HL, Griffin M, Hony S, Isaak KG, Levenson LR, Lu N, Madden S, O'Halloran B, Okumura K, Oliver S, Page MJ, Panuzzo P, Papageorgiou A, Parkin TJ, Perez-Fournon I, Pohlen M, Rangwala N, Rigby EE, Roussel H, Rykala A, Sacchi N, Sauvage M, Schulz B, Schirm MRP, Smith MWL, Spinoglio L, Stevens JA, Srinivasan S, Symeonidis M, Trichas M, Vaccari M, Vigroux L, Wozniak H, Wright GS, Zeilinger WW (2010) On the origin of M81 group extended dust emission. *MNRAS* 409:102–108, DOI 10.1111/j.1365-2966.2010.17774.x, 1010.4770
- de Jong RS (2008) Point spread function tails and the measurements of diffuse stellar halo light around edge-on disc galaxies. *MNRAS* 388:1521–1527, DOI 10.1111/j.1365-2966.2008.13505.x, 0807.0229
- Duc PA, Cuillandre JC, Karabal E, Cappellari M, Alatalo K, Blitz L, Bournaud F, Bureau M, Crocker AF, Davies RL, Davis TA, de Zeeuw PT, Emsellem E, Khochfar S, Krajnović D, Kuntschner H, McDermid RM, Michel-Dansac L, Morganti R, Naab T, Oosterloo T, Paudel S, Sarzi M, Scott N, Serra P, Weijmans AM, Young LM (2015) The ATLAS^{3D} project - XXIX. The new look of early-type galaxies and surrounding fields disclosed by extremely deep optical images. *MNRAS* 446:120–143, DOI 10.1093/mnras/stu2019, 1410.0981
- Durrell PR, Côté P, Peng EW, Blakeslee JP, Ferrarese L, Mihos JC, Puzia TH, Lançon A, Liu C, Zhang H, Cuillandre JC, McConnachie A, Jordán A, Accetta K, Boissier S, Boselli A, Courteau S, Duc PA, Emsellem E, Gwyn S, Mei S, Taylor JE (2014) The Next Generation Virgo Cluster Survey. VIII. The Spatial Distribution of Globular Clusters in the Virgo Cluster. *ApJ* 794:103, DOI 10.1088/0004-637X/794/2/103, 1408.2821
- Elmegreen BG, Elmegreen DM (2006) Observations of Thick Disks in the Hubble Space Telescope Ultra Deep Field. *ApJ* 650:644–660, DOI 10.1086/507578, astro-ph/0607540
- Ferguson AMN, Mackey AD (2016) Substructure and Tidal Streams in the Andromeda Galaxy and its Satellites. In: Newberg HJ, Carlin JL (eds) *Astrophysics and Space Science Library*, *Astrophysics and Space Science Library*, vol 420, p 191, DOI 10.1007/978-3-319-19336-6_8, 1603.01993
- Ferrarese L, Côté P, Cuillandre JC, Gwyn SDJ, Peng EW, MacArthur LA, Duc PA, Boselli A, Mei S, Erben T, McConnachie AW, Durrell PR, Mihos JC, Jordán A, Lançon A, Puzia TH, Emsellem E, Balogh ML, Blakeslee JP, van Waerbeke L, Gavazzi R, Vollmer B, Kavelaars JJ, Woods D, Ball NM, Boissier S, Courteau S, Ferriere E, Gavazzi G, Hildebrandt H, Hudelot P, Huertas-Company M, Liu C, McLaughlin D, Mellier Y, Milkeraitis M, Schade D, Balkowski C, Bournaud F, Carlberg RG, Chapman SC, Hoekstra H, Peng C, Sawicki M, Simard L, Taylor

- JE, Tully RB, van Driel W, Wilson CD, Burdullis T, Mahoney B, Manset N (2012) The Next Generation Virgo Cluster Survey (NGVS). I. Introduction to the Survey. *ApJS* 200:4, DOI 10.1088/0067-0049/200/1/4
- Fliri J, Trujillo I (2016) The IAC Stripe 82 Legacy Project: a wide-area survey for faint surface brightness astronomy. *MNRAS* 456:1359–1373, DOI 10.1093/mnras/stv2686, 1603.04474
- Font AS, McCarthy IG, Crain RA, Theuns T, Schaye J, Wiersma RPC, Dalla Vecchia C (2011) Cosmological simulations of the formation of the stellar haloes around disc galaxies. *MNRAS* 416:2802–2820, DOI 10.1111/j.1365-2966.2011.19227.x, 1102.2526
- Freeman KC (1970) On the Disks of Spiral and S0 Galaxies. *ApJ* 160:811, DOI 10.1086/150474
- Galaz G, Milovic C, Suc V, Busta L, Lizana G, Infante L, Royo S (2015) Deep Optical Images of Malin 1 Reveal New Features. *ApJL* 815:L29, DOI 10.1088/2041-8205/815/2/L29, 1512.01095
- Gallart C, Monelli M, Mayer L, Aparicio A, Battaglia G, Bernard EJ, Cassisi S, Cole AA, Dolphin AE, Drozdovsky I, Hidalgo SL, Navarro JF, Salvadori S, Skillman ED, Stetson PB, Weisz DR (2015) The ACS LCID Project: On the Origin of Dwarf Galaxy Types—A Manifestation of the Halo Assembly Bias? *ApJL* 811:L18, DOI 10.1088/2041-8205/811/2/L18, 1507.08350
- Gilbert KM, Guhathakurta P, Beaton RL, Bullock J, Geha MC, Kalirai JS, Kirby EN, Majewski SR, Osthheimer JC, Patterson RJ, Tollerud EJ, Tanaka M, Chiba M (2012) Global Properties of M31's Stellar Halo from the SPLASH Survey. I. Surface Brightness Profile. *ApJ* 760:76, DOI 10.1088/0004-637X/760/1/76, 1210.3362
- Gilmore G, Reid N (1983) New light on faint stars. III - Galactic structure towards the South Pole and the Galactic thick disc. *MNRAS* 202:1025–1047, DOI 10.1093/mnras/202.4.1025
- Gilmore G, Wyse RFG (1985) The abundance distribution in the inner spheroid. *AJ* 90:2015–2026, DOI 10.1086/113907
- Guérou A, Emsellem E, Krajnović D, McDermid RM, Contini T, Weillbacher PM (2016) Exploring the mass assembly of the early-type disc galaxy NGC 3115 with MUSE. *A&A* 591:A143, DOI 10.1051/0004-6361/201628743, 1605.07667
- Gunn JE, Carr M, Rockosi C, Sekiguchi M, Berry K, Elms B, de Haas E, Ivezić Ž, Knapp G, Lupton R, Pauls G, Simcoe R, Hirsch R, Sanford D, Wang S, York D, Harris F, Annis J, Bartoček L, Boroski W, Bakken J, Haldeman M, Kent S, Holm S, Holmgren D, Petravick D, Prossapio A, Rechenmacher R, Doi M, Fukugita M, Shimasaku K, Okada N, Hull C, Siegmund W, Mannery E, Blouke M, Heidtman D, Schneider D, Lucinio R, Brinkman J (1998) The Sloan Digital Sky Survey Photometric Camera. *AJ* 116:3040–3081, DOI 10.1086/300645, astro-ph/9809085
- Haywood M, Di Matteo P, Lehnert MD, Katz D, Gómez A (2013) The age structure of stellar populations in the solar vicinity. Clues of a two-phase formation history of the Milky Way disk. *A&A* 560:A109, DOI 10.1051/0004-6361/201321397, 1305.4663
- Howell SB (2006) *Handbook of CCD Astronomy*, 2nd ed. Cambridge observing handbooks for research astronomers, Vol. 5 Cambridge, UK: Cambridge University Press, 2006 ISBN 0521852153
- Ibata R, Irwin M, Lewis G, Ferguson AMN, Tanvir N (2001) A giant stream of metal-rich stars in the halo of the galaxy M31. *Nature* 412:49–52, astro-ph/0107090
- Ibata R, Martin NF, Irwin M, Chapman S, Ferguson AMN, Lewis GF, McConnachie AW (2007) The Haunted Halos of Andromeda and Triangulum: A Panorama of Galaxy Formation in Action. *ApJ* 671:1591–1623, DOI 10.1086/522574, 0704.1318
- Irwin MJ, Ferguson AMN, Ibata RA, Lewis GF, Tanvir NR (2005) A Minor-Axis Surface Brightness Profile for M31. *ApJL* 628:L105–L108, DOI 10.1086/432718, astro-ph/0505077
- Ivezić Z, Axelrod T, Brandt WN, Burke DL, Claver CF, Connolly A, Cook KH, Gee P, Gilmore DK, Jacoby SH, Jones RL, Kahn SM, Kantor JP, Krabbendam VV, Lupton RH, Monet DG, Pinto PA, Saha A, Schalk TL, Schneider DP, Strauss MA, Stubbs CW, Sweeney D, Szalay A, Thaler JJ, Tyson JA, LSST Collaboration (2008) Large Synoptic Survey Telescope: From Science Drivers To Reference Design. *Serbian Astronomical Journal* 176:1–13, DOI 10.2298/SAJ0876001I

- Jablonka P, Tafelmeyer M, Courbin F, Ferguson AMN (2010) Direct detection of galaxy stellar halos: NGC 3957 as a test case. *A&A* 513:A78, DOI 10.1051/0004-6361/200913320, 1001.3067
- Javanmardi B, Martinez-Delgado D, Kroupa P, Henkel C, Crawford K, Teuwen K, Gabany RJ, Hanson M, Chonis TS, Neyer F (2016) DGSAT: Dwarf Galaxy Survey with Amateur Telescopes. I. Discovery of low surface brightness systems around nearby spiral galaxies. *A&A* 588:A89, DOI 10.1051/0004-6361/201527745, 1511.04446
- Jiang L, Fan X, Annis J, Becker RH, White RL, Chiu K, Lin H, Lupton RH, Richards GT, Strauss MA, Jester S, Schneider DP (2008) A Survey of $z \sim 6$ Quasars in the Sloan Digital Sky Survey Deep Stripe. I. A Flux-Limited Sample at $z_{AB} < 21$. *AJ* 135:1057–1066, DOI 10.1088/0004-6256/135/3/1057, 0708.2578
- Jiang L, Fan X, Bian F, McGreer ID, Strauss MA, Annis J, Buck Z, Green R, Hodge JA, Myers AD, Rafiee A, Richards G (2014) The Sloan Digital Sky Survey Stripe 82 Imaging Data: Depth-optimized Co-adds over 300 deg² in Five Filters. *ApJS* 213:12, DOI 10.1088/0067-0049/213/1/12, 1405.7382
- Johnston KV, Bullock JS, Sharma S, Font A, Robertson BE, Leitner SN (2008) Tracing Galaxy Formation with Stellar Halos. II. Relating Substructure in Phase and Abundance Space to Accretion Histories. *ApJ* 689:936–957, DOI 10.1086/592228, 0807.3911
- Kasparova AV, Katkov IY, Chilingarian IV, Silchenko OK, Moiseev AV, Borisov SB (2016) The diversity of thick galactic discs. *MNRAS* 460:L89–L93, DOI 10.1093/mnras/lfw083, 1604.07624
- Kawata D, Chiappini C (2016) Milky Way's thick and thin disk: Is there a distinct thick disk? *Astronomische Nachrichten* 337:976, DOI 10.1002/asna.201612421, 1608.01698
- Klypin A, Kravtsov AV, Valenzuela O, Prada F (1999) Where Are the Missing Galactic Satellites? *ApJ* 522:82–92, DOI 10.1086/307643, astro-ph/9901240
- Kregel M, van der Kruit PC, de Grijs R (2002) Flattening and truncation of stellar discs in edge-on spiral galaxies. *MNRAS* 334:646–668, DOI 10.1046/j.1365-8711.2002.05556.x, astro-ph/0204154
- Liu L, Gerke BF, Wechsler RH, Behroozi PS, Busha MT (2011) How Common are the Magellanic Clouds? *ApJ* 733:62, DOI 10.1088/0004-637X/733/1/62, 1011.2255
- Majewski SR, Skrutskie MF, Weinberg MD, Ostheimer JC (2003) A Two Micron All Sky Survey View of the Sagittarius Dwarf Galaxy. I. Morphology of the Sagittarius Core and Tidal Arms. *ApJ* 599:1082–1115, DOI 10.1086/379504, astro-ph/0304198
- Martín-Navarro I, Bakos J, Trujillo I, Knapen JH, Athanassoula E, Bosma A, Comerón S, Elmegreen BG, Erroz-Ferrer S, Gadotti DA, Gil de Paz A, Hinz JL, Ho LC, Holwerda BW, Kim T, Laine J, Laurikainen E, Menéndez-Delmestre K, Mizusawa T, Muñoz-Mateos JC, Regan MW, Salo H, Seibert M, Sheth K (2012) A unified picture of breaks and truncations in spiral galaxies from SDSS and S⁴G imaging. *MNRAS* 427:1102–1134, DOI 10.1111/j.1365-2966.2012.21929.x, 1208.2893
- Martín-Navarro I, Trujillo I, Knapen JH, Bakos J, Fliri J (2014) Stellar haloes outshine disc truncations in low-inclined spirals. *MNRAS* 441:2809–2814, DOI 10.1093/mnras/stu767, 1401.3749
- Martínez-Delgado D, Peñarrubia J, Gabany RJ, Trujillo I, Majewski SR, Pohlen M (2008) The Ghost of a Dwarf Galaxy: Fossils of the Hierarchical Formation of the Nearby Spiral Galaxy NGC 5907. *ApJ* 689:184–193, DOI 10.1086/592555, 0805.1137
- Martínez-Delgado D, Gabany RJ, Crawford K, Zibetti S, Majewski SR, Rix HW, Fliri J, Carballo-Bello JA, Bardalez-Gagliuffi DC, Peñarrubia J, Chonis TS, Madore B, Trujillo I, Schirmer M, McDavid DA (2010) Stellar Tidal Streams in Spiral Galaxies of the Local Volume: A Pilot Survey with Modest Aperture Telescopes. *AJ* 140:962–967, DOI 10.1088/0004-6256/140/4/962, 1003.4860
- Martínez-Delgado D, D'Onghia E, Chonis TS, Beaton RL, Teuwen K, Gabany RJ, Grebel EK, Morales G (2015) A Stellar Tidal Stream Around the Whale Galaxy, NGC 4631. *AJ* 150:116, DOI 10.1088/0004-6256/150/4/116, 1410.6368

- McConnachie AW (2012) The Observed Properties of Dwarf Galaxies in and around the Local Group. *AJ* 144:4, DOI 10.1088/0004-6256/144/1/4, 1204.1562
- McConnachie AW, Irwin MJ, Ibata RA, Dubinski J, Widrow LM, Martin NF, Côté P, Dotter AL, Navarro JF, Ferguson AMN, Puzia TH, Lewis GF, Babul A, Barmby P, Bienaymé O, Chapman SC, Cockcroft R, Collins MLM, Fardal MA, Harris WE, Huxor A, Mackey AD, Peñarrubia J, Rich RM, Richer HB, Siebert A, Tanvir N, Valls-Gabaud D, Venn KA (2009) The remnants of galaxy formation from a panoramic survey of the region around M31. *Nature* 461:66–69, DOI 10.1038/nature08327, 0909.0398
- McGraw JT, Angel JRP, Sargent TA (1980) A charge-coupled device /CCD/ transit-telescope survey for galactic and extragalactic variability and polarization. In: Elliott DA (ed) Conference on Applications of Digital Image Processing to Astronomy, Proc. SPIE, vol 264, pp 20–28
- Merritt A, van Dokkum P, Abraham R, Zhang J (2016) The Dragonfly nearby Galaxies Survey. I. Substantial Variation in the Diffuse Stellar Halos around Spiral Galaxies. *ApJ* 830:62, DOI 10.3847/0004-637X/830/2/62, 1606.08847
- Mihos JC, Harding P, Feldmeier J, Morrison H (2005) Diffuse Light in the Virgo Cluster. *ApJL* 631:L41–L44, DOI 10.1086/497030, astro-ph/0508217
- Mihos JC, Harding P, Spengler CE, Rudick CS, Feldmeier JJ (2013) The Extended Optical Disk of M101. *ApJ* 762:82, DOI 10.1088/0004-637X/762/2/82, 1211.3095
- Mihos JC, Durrell PR, Ferrarese L, Feldmeier JJ, Côté P, Peng EW, Harding P, Liu C, Gwyn S, Cuillandre JC (2015) Galaxies at the Extremes: Ultra-diffuse Galaxies in the Virgo Cluster. *ApJL* 809:L21, DOI 10.1088/2041-8205/809/2/L21, 1507.02270
- Mihos JC, Harding P, Feldmeier JJ, Rudick C, Janowiecki S, Morrison H, Slater C, Watkins A (2016) The Burrell Schmidt Deep Virgo Survey: Tidal Debris, Galaxy Halos, and Diffuse Intracluster Light in the Virgo Cluster. *ArXiv e-prints* 1611.04435
- Monachesi A, Bell EF, Radburn-Smith DJ, Bailin J, de Jong RS, Holwerda B, Streich D, Silverstein G (2016) The GHOSTS survey - II. The diversity of halo colour and metallicity profiles of massive disc galaxies. *MNRAS* 457:1419–1446, DOI 10.1093/mnras/stv2987, 1507.06657
- Moore B, Ghigna S, Governato F, Lake G, Quinn T, Stadel J, Tozzi P (1999) Dark Matter Substructure within Galactic Halos. *ApJL* 524:L19–L22, DOI 10.1086/312287, astro-ph/9907411
- Mould J (2005) Red Thick Disks of Nearby Galaxies. *AJ* 129:698–711, DOI 10.1086/427248, astro-ph/0411231
- Navarro JF, Eke VR, Frenk CS (1996) The cores of dwarf galaxy haloes. *MNRAS* 283:L72–L78, DOI 10.1093/mnras/283.3.L72, astro-ph/9610187
- Peters SPC, van der Kruit PC, Knapen JH, Trujillo I, Fliri J, Cisternas M, Kelvin LS (2017) Stellar Disc Truncations and Extended Haloes in Face-on Spiral Galaxies. *MNRAS*, submitted
- Pillepich A, Vogelsberger M, Deason A, Rodriguez-Gomez V, Genel S, Nelson D, Torrey P, Sales LV, Marinacci F, Springel V, Sijacki D, Hernquist L (2014) Halo mass and assembly history exposed in the faint outskirts: the stellar and dark matter haloes of Illustris galaxies. *MNRAS* 444:237–249, DOI 10.1093/mnras/stu1408, 1406.1174
- Pohlen M, Trujillo I (2006) The structure of galactic disks. Studying late-type spiral galaxies using SDSS. *A&A* 454:759–772, DOI 10.1051/0004-6361:20064883, astro-ph/0603682
- Purcell CW, Bullock JS, Zentner AR (2007) Shredded Galaxies as the Source of Diffuse Intrahalo Light on Varying Scales. *ApJ* 666:20–33, DOI 10.1086/519787, astro-ph/0703004
- Quinn PJ, Hernquist L, Fullagar DP (1993) Heating of galactic disks by mergers. *ApJ* 403:74–93, DOI 10.1086/172184
- Radburn-Smith DJ, de Jong RS, Seth AC, Bailin J, Bell EF, Brown TM, Bullock JS, Courteau S, Dalcanton JJ, Ferguson HC, Goudfrooij P, Holfeltz S, Holwerda BW, Purcell C, Sick J, Streich D, Vlajic M, Zucker DB (2011) The GHOSTS Survey. I. Hubble Space Telescope Advanced Camera for Surveys Data. *ApJS* 195:18, DOI 10.1088/0067-0049/195/2/18
- Read JI, Gilmore G (2005) Mass loss from dwarf spheroidal galaxies: the origins of shallow dark matter cores and exponential surface brightness profiles. *MNRAS* 356:107–124, DOI 10.1111/j.1365-2966.2004.08424.x, astro-ph/0409565

- Read JI, Wilkinson MI, Evans NW, Gilmore G, Kleyna JT (2006) The importance of tides for the Local Group dwarf spheroidals. *MNRAS* 367:387–399, DOI 10.1111/j.1365-2966.2005.09959.x, astro-ph/0511759
- Rejkuba M, Mouhcine M, Ibata R (2009) The stellar population content of the thick disc and halo of the Milky Way analogue NGC 891. *MNRAS* 396:1231–1246, DOI 10.1111/j.1365-2966.2009.14821.x, 0903.4211
- Rudick CS, Mihos JC, Harding P, Feldmeier JJ, Janowiecki S, Morrison HL (2010) Optical Colors of Intracluster Light in the Virgo Cluster Core. *ApJ* 720:569–580, DOI 10.1088/0004-637X/720/1/569, 1003.4500
- Ruiz P, Trujillo I, Mármod-Queraltó E (2015) The abundance of satellites depends strongly on the morphology of the host galaxy. *MNRAS* 454:1605–1619, DOI 10.1093/mnras/stv2030, 1504.02777
- Samland M, Gerhard OE (2003) The formation of a disk galaxy within a growing dark halo. *A&A* 399:961–982, DOI 10.1051/0004-6361/20021842, astro-ph/0301499
- Sandin C (2014) The influence of diffuse scattered light. I. The PSF and its role in observations of the edge-on galaxy NGC 5907. *A&A* 567:A97, DOI 10.1051/0004-6361/201423429, 1406.5508
- Sandin C (2015) The influence of diffuse scattered light. II. Observations of galaxy haloes and thick discs and hosts of blue compact galaxies. *A&A* 577:A106, DOI 10.1051/0004-6361/201425168, 1502.07244
- Schönrich R, Binney J (2009) Chemical evolution with radial mixing. *MNRAS* 396:203–222, DOI 10.1111/j.1365-2966.2009.14750.x, 0809.3006
- Seth AC, Dalcanton JJ, de Jong RS (2005) A Study of Edge-On Galaxies with the Hubble Space Telescope Advanced Camera for Surveys. II. Vertical Distribution of the Resolved Stellar Population. *AJ* 130:1574–1592, DOI 10.1086/444620, astro-ph/0506117
- Sheth K, Regan M, Hinz JL, Gil de Paz A, Menéndez-Delmestre K, Muñoz-Mateos JC, Seibert M, Kim T, Laurikainen E, Salo H, Gadotti DA, Laine J, Mizusawa T, Armus L, Athanassoula E, Bosma A, Buta RJ, Capak P, Jarrett TH, Elmegreen DM, Elmegreen BG, Knapen JH, Koda J, Helou G, Ho LC, Madore BF, Masters KL, Mobasher B, Ogle P, Peng CY, Schinnerer E, Surace JA, Zaritsky D, Comerón S, de Swardt B, Meidt SE, Kasliwal M, Aravena M (2010) The Spitzer Survey of Stellar Structure in Galaxies (S^4G). *PASP* 122:1397–1414, DOI 10.1086/657638, 1010.1592
- Slater CT, Harding P, Mihos JC (2009) Removing Internal Reflections from Deep Imaging Data Sets. *PASP* 121:1267–1278, DOI 10.1086/648457, 0909.3320
- Streich D, de Jong RS, Bailin J, Bell EF, Holwerda BW, Minchev I, Monachesi A, Radburn-Smith DJ (2016) Extragalactic archeology with the GHOSTS Survey. I. Age-resolved disk structure of nearby low-mass galaxies. *A&A* 585:A97, DOI 10.1051/0004-6361/201526013, 1509.06647
- Tanaka M, Chiba M, Komiyama Y, Guhathakurta P, Kalirai JS, Iye M (2010) Structure and Population of the Andromeda Stellar Halo from a Subaru/Suprime-Cam Survey. *ApJ* 708:1168–1203, DOI 10.1088/0004-637X/708/2/1168, 0908.0245
- Tikhonov NA, Galazutdinova OA (2005) Stellar Disks and Halos of Edge-on Spiral Galaxies: NGC 891, NGC 4144, and NGC 4244. *Astrophysics* 48:221–236, DOI 10.1007/s10511-005-0021-8, astro-ph/0503235
- Tissera PB, Beers TC, Carollo D, Scannapieco C (2014) Stellar haloes in Milky Way mass galaxies: from the inner to the outer haloes. *MNRAS* 439:3128–3138, DOI 10.1093/mnras/stu181, 1309.3609
- Trujillo I, Fliri J (2016) Beyond 31 mag arcsec²: The Frontier of Low Surface Brightness Imaging with the Largest Optical Telescopes. *ApJ* 823:123, DOI 10.3847/0004-637X/823/2/123, 1510.04696
- Tsikoudi V (1979) Photometry and structure of lenticular galaxies. I - NGC 3115. *ApJ* 234:842–853, DOI 10.1086/157565
- van der Kruit PC (1979) Optical surface photometry of eight spiral galaxies studied in Westerbork. *A&AS* 38:15–38

- van der Kruit PC, Freeman KC (2011) Galaxy Disks. *ARAA* 49:301–371, DOI 10.1146/annurev-astro-083109-153241, 1101.1771
- van der Kruit PC, Searle L (1981) Surface photometry of edge-on spiral galaxies. I - A model for the three-dimensional distribution of light in galactic disks. *A&A* 95:105–115
- van Dokkum P, Abraham R, Brodie J, Conroy C, Danieli S, Merritt A, Mowla L, Romanowsky A, Zhang J (2016) A High Stellar Velocity Dispersion and ~100 Globular Clusters for the Ultra-diffuse Galaxy Dragonfly 44. *ApJL* 828:L6, DOI 10.3847/2041-8205/828/1/L6, 1606.06291
- van Dokkum PG, Abraham R, Merritt A (2014) First Results from the Dragonfly Telephoto Array: The Apparent Lack of a Stellar Halo in the Massive Spiral Galaxy M101. *ApJL* 782:L24, DOI 10.1088/2041-8205/782/2/L24, 1401.5467
- Villumsen JV (1985) Evolution of the velocity distribution in galactic disks. *ApJ* 290:75–85, DOI 10.1086/162960
- Watkins AE, Mihos JC, Harding P, Feldmeier JJ (2014) Searching for Diffuse Light in the M96 Galaxy Group. *ApJ* 791:38, DOI 10.1088/0004-637X/791/1/38, 1406.6982
- Wright JF, Mackay CD (1981) The Cambridge Charge-Coupled Device / CCD / System. In: Society of Photo-Optical Instrumentation Engineers (SPIE) Conference Series, Proc. SPIE, vol 290, p 160
- Yoachim P, Dalcanton JJ (2006) Structural Parameters of Thin and Thick Disks in Edge-on Disk Galaxies. *AJ* 131:226–249, DOI 10.1086/497970, astro-ph/0508460
- York DG, Adelman J, Anderson JE Jr, Anderson SF, Annis J, Bahcall NA, Bakken JA, Barkhouser R, Bastian S, Berman E, Boroski WN, Bracker S, Briegel C, Briggs JW, Brinkmann J, Brunner R, Burles S, Carey L, Carr MA, Castander FJ, Chen B, Colestock PL, Connolly AJ, Crocker JH, Csabai I, Czarapata PC, Davis JE, Doi M, Dombeck T, Eisenstein D, Ellman N, Elms BR, Evans ML, Fan X, Federwitz GR, Fiscelli L, Friedman S, Frieman JA, Fukugita M, Gillespie B, Gunn JE, Gurbani VK, de Haas E, Haldeman M, Harris FH, Hayes J, Heckman TM, Hennessy GS, Hindsley RB, Holm S, Holmgren DJ, Huang Ch, Hull C, Husby D, Ichikawa SI, Ichikawa T, Ivezić Ž, Kent S, Kim RSJ, Kinney E, Klaene M, Kleinman AN, Kleinman S, Knapp GR, Korienek J, Kron RG, Kunszt PZ, Lamb DQ, Lee B, Leger RF, Limmongkol S, Lindenmeyer C, Long DC, Loomis C, Loveday J, Lucinio R, Lupton RH, MacKinnon B, Mannery EJ, Mantsch PM, Margon B, McGehee P, McKay TA, Meiksin A, Merelli A, Monet DG, Munn JA, Narayanan VK, Nash T, Neilsen E, Neswold R, Newberg HJ, Nichol RC, Nicinski T, Nonino M, Okada N, Okamura S, Ostriker JP, Owen R, Pauls AG, Peoples J, Peterson RL, Petravick D, Pier JR, Pope A, Pordes R, Prosapio A, Rechenmacher R, Quinn TR, Richards GT, Richmond MW, Rivetta CH, Rockosi CM, Ruthmansdorfer K, Sandford D, Schlegel DJ, Schneider DP, Sekiguchi M, Sergey G, Shimasaku K, Siegmund WA, Smee S, Smith JA, Snedden S, Stone R, Stoughton C, Strauss MA, Stubbs C, SubbaRao M, Szalay AS, Szapudi I, Szokoly GP, Thakar AR, Tremonti C, Tucker DL, Uomoto A, Vanden Berk D, Vogeley MS, Waddell P, Wang Si, Watanabe M, Weinberg DH, Yanny B, Yasuda N, SDSS Collaboration (2000) The Sloan Digital Sky Survey: Technical Summary. *AJ* 120:1579–1587, DOI 10.1086/301513, astro-ph/0006396
- Yoshii Y (1982) Density Distribution of Faint Stars in the Direction of the North Galactic Pole. *PASJ* 34:365
- Zackrisson E, de Jong RS, Micheva G (2012) Unlocking the secrets of stellar haloes using combined star counts and surface photometry. *MNRAS* 421:190–201, DOI 10.1111/j.1365-2966.2011.20290.x, 1112.1696
- Zaritsky D, Salo H, Laurikainen E, Elmegreen D, Athanassoula E, Bosma A, Comerón S, Erroz-Ferrer S, Elmegreen B, Gadotti DA, Gil de Paz A, Hinz JL, Ho LC, Holwerda BW, Kim T, Knapen JH, Laine J, Laine S, Madore BF, Meidt S, Menendez-Delmestre K, Mizusawa T, Muñoz-Mateos JC, Regan MW, Seibert M, Sheth K (2013) On the Origin of Lopsidedness in Galaxies as Determined from the Spitzer Survey of Stellar Structure in Galaxies (S⁴G). *ApJ* 772:135, DOI 10.1088/0004-637X/772/2/135, 1305.2940